Electronic Supplementary Material (ESI) for Chemical Communications

Supporting Information

The self-complexation of mono-urea-functionalized pillar[5]arenes with abnormal urea behaviors

Mengfei Ni, Xiaoyu Hu*, Juli Jiang*, and Leyong Wang

Key Laboratory of Mesoscopic Chemistry of MOE, Center for Multimolecular Chemistry, School of Chemistry and Chemical Engineering, Nanjing University, Nanjing 210093, China. E-mail: huxy@nju.edu.cn; jjl@nju.edu.cn; Fax: +86 025 83597090; Tel: +86 025 83592529.

Table of Contents

Materials and methods

All reagents were commercially available and most of them were used without further purification, except that some solvents were dried by standard methods. All reactions were performed in atmosphere unless noted. NMR spectra were recorded on a Bruker DPX 300 spectrometer or a Bruker Avance III 400 spectrometer with TMS as the internal standard. COSY, NOESY and DOSY experiments were performed on a Bruker Avance III 400 spectrometer. Electrospray ionization mass spectra (ESI-MS) were acquired on a Finnigan Mat TSQ 7000 instrument. High-resolution electrospray ionization mass spectra (HR-ESI-MS) were recorded on an Agilent 6540Q-TOF LCMS equipped with an electrospray ionization (ESI) probe operating in positive-ion mode with direct infusion. The melting points were collected on an X-4 digital melting point apparatus without correction. FTIR spectra were recorded on an FTIR Bruker Tensor 27 infrared spectrophotometer. Single crystal X-ray data were obtained on a Bruker SMART APEX II CCD diffractometer (Mo Kα radiation, $\lambda = 0.71073$ Å). Structure solutions and refinements were carried out using the SHELXTL-PC software package.[S1]

Compounds **3a** and **3b** were synthesized according to the literatures.[S2]

Synthesis of ***2a***, ***2b***, ***1b***, *and* ***1c***

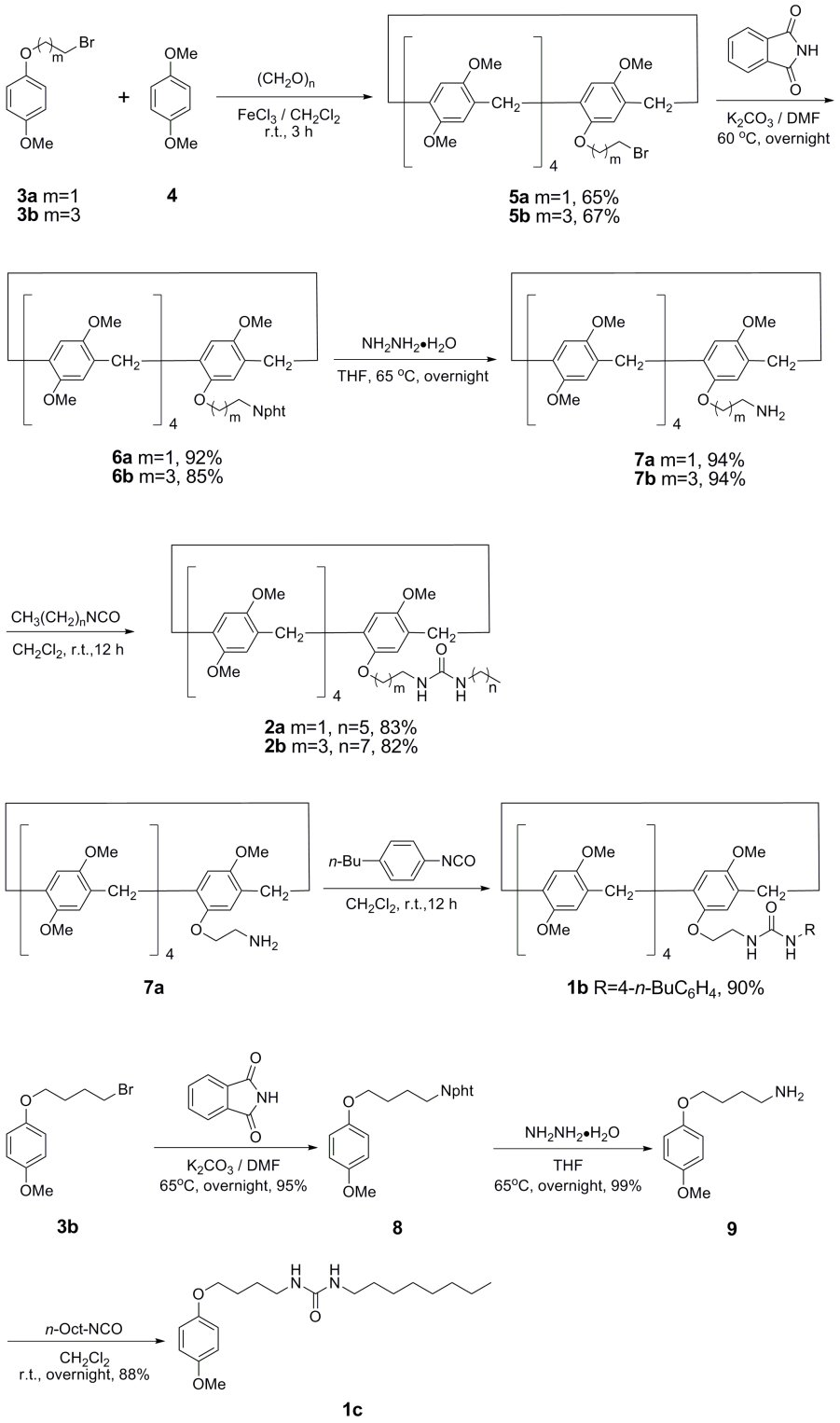

Scheme S1 Synthetic route for compounds **2a**, **2b**, **1b**, and **1c**.

General procedure for the synthesis of pillar[5]arene 5:[S3] Compound **3** (1.50 mmol) and **4** (3.32 g, 24.0 mmol) were dissolved in dry dichloromethane (500 mL), and then paraformaldehyde (2.16 g, 72.0 mmol) was added to the solution. After stirred for 10 min, anhydrous ferric chloride (0.623 g, 3.84 mmol) was added. The reaction mixture was stirred for 3 h at room temperature under argon atmosphere, and then water (300 mL) was added to the mixture. The organic phase was separated and dried over anhydrous Na_2SO_4. Then the solvent was removed and the crude product was purified by column chromatography (silica, *n*-hexane/CH_2Cl_2 = 1/2).

5a[S4]: White solid, 0.82 g, 0.97 mmol, 65%.

5b[S3]: White solid, 0.87 g, 1.0 mmol, 67%.

General procedure for the synthesis of pillar[5]arene 6: To a solution of compound **5** (1.00 mmol) in dry DMF (10 mL) was added phthalimide (0.21 g, 1.43 mmol) and K_2CO_3 (0.22 g, 1.60 mmol) at room temperature. The reaction mixture was stirred overnight at 60 ^oC. After cooling, the solvent was removed under vacuum. Then water (40 mL) was added to the resulting mixture, and extracted with CH_2Cl_2 (2 × 40 mL). The organic layer was dried over anhydrous Na_2SO_4 and concentrated under reduced pressure. The crude product was purified by column chromatography (silica, CH_2Cl_2).

6a: Yellow solid, 0.83 g, 0.91 mmol, 92%. M.p. 65–67 ^oC. ^1H NMR (300 MHz, $CDCl_3$, 298 K) δ (ppm): 7.84–7.87 (m, 2H, Ar), 7.70–7.73 (m, 2H, Ar), 6.71–6.91 (m, 10H, Ar), 4.12 (t, J = 4.3 Hz, 2H, CH_2), 3.58–3.78 (m, 39H, CH_2, CH_3). ^{13}C NMR (75 MHz, $CDCl_3$, 298 K) δ (ppm): 168.3, 151.2, 151.04, 150.96, 150.9, 149.6, 134.1, 132.2, 128.4, 128.33, 128.28, 128.2, 128.1, 123.4, 114.7, 114.3, 114.2, 114.0, 65.5, 56.03, 55.96, 55.9, 55.8, 38.0, 29.8, 29.6. ESI-MS: *m/z* 927.2 $[M+NH_4]^+$ (100%). HR-ESI-MS: *m/z* calcd for $[M+Na]^+$ $C_{54}H_{55}NO_{12}Na$, 932.3616, found 932.3615.

6b: Yellow solid, 0.80 g, 0.85 mmol, 85%. M.p. 73–74 ^oC. ^1H NMR (300 MHz, $CDCl_3$, 298 K) δ (ppm): 7.84–7.87 (m, 2H, Ar), 7.71–7.74 (m, 2H, Ar), 6.69–6.77 (m, 10H, Ar), 3.86 (t, J = 6.0 Hz, 2H, CH_2), 3.75–3.80 (m, 12H, CH_2), 3.58–3.64 (m, 27H, CH_3), 1.81–1.96 (m, 4H, CH_2). ^{13}C NMR (75 MHz, $CDCl_3$, 298 K) δ (ppm): 168.5,

150.9, 150.1, 134.5, 134.1, 132.2, 128.5, 128.3, 123.8, 123.3, 115.2, 114.3, 114.25, 114.16, 114.1, 68.0, 55.9, 55.8, 37.9, 29.9, 29.8, 29.6, 27.3, 25.7. ESI-MS: *m/z* 955.4 $[M+NH_4]^+$ (100%). HR-ESI-MS: *m/z* calcd for $[M+Na]^+$ $C_{56}H_{59}NO_{12}Na$, 960.3929, found 960.3931.

General procedure for the synthesis of pillar[5]arene 7: Compound **6** (0.38 mmol) was dissolved in THF (20 mL). The solution was heated to 65 °C and hydrazine monohydrate (85%, 0.22 mL, 3.8 mmol) was added. The reaction mixture was stirred overnight under argon atmosphere. After cooling, the solvent was removed. Then saturated aqueous Na_2CO_3 (30 mL) was added to the resulting mixture, and extracted with CH_2Cl_2 (2 × 30 mL). The organic layer was combined and dried over anhydrous Na_2SO_4 and concentrated under reduced pressure to give the product without further purification.

7a: White solid, 0.28 g, 0.36 mmol, 94%. M.p. 48–50 °C. ^{1}H NMR (300 MHz, DMSO-d_6, 298 K): δ (ppm): 6.72–6.81 (m, 10H, Ar), 3.76 (t, J = 5.7 Hz, 2H, CH_2), 3.64–3.66 (m, 37H, CH_2, CH_3), 2.86 (t, J = 5.6 Hz, 2H, CH_2), 1.67 (br, 2H, NH_2). ^{13}C NMR (75 MHz, DMSO-d_6, 298 K): δ (ppm):149.93, 149.89, 149.86, 149.2, 127.5, 114.1, 113.5, 113.4, 113.3, 70.5, 55.4, 41.3, 29.1, 29.0, 28.9. ESI-MS: *m/z* 780.4 $[M+H]^+$ (100%). HR-ESI-MS: *m/z* calcd for $[M+H]^+$ $C_{46}H_{54}NO_{10}$, 780.3742, found 780.4017.

7b: White solid, 0.29 g, 0.36 mmol, 94%. M.p. 114–115 °C. ^{1}H NMR (400 MHz, DMSO-d_6, 298 K): δ (ppm): 6.74–6.80 (m, 10H, Ar), 3.81 (t, J = 6.3 Hz, 2H, CH_2), 3.65 (br, 37H, CH_2, CH_3), 2.57 (t, J = 6.9 Hz, 2H, CH_2), 1.70–1.77 (m, 2H, CH_2), 1.48–1.56 (m, 2H, CH_2). ^{13}C NMR (100 MHz, DMSO-d_6, 298 K): δ (ppm): 150.0, 149.92, 149.87, 149.3, 127.51, 127.47, 127.4, 114.1, 113.3, 67.7, 55.42, 55.37, 28.9, 26.6. ESI-MS: *m/z* 808.5 $[M+H]^+$ (100%). HR-ESI-MS: *m/z* calcd for $[M+H]^+$ $C_{48}H_{58}NO_{10}$, 808.4055, found 808.4063.

General procedure for the synthesis of 1b, **2a and 2b**: To a solution of compound **7** (1.26 mmol) in dry CH_2Cl_2 (30 mL) was added the isocyanate (1.51

mmol) under argon atmosphere. The reaction mixture was stirred for 12 h at room temperature. After the solvent was removed under vacuum, the crude product was purified by column chromatography (silica, CH_2Cl_2/MeOH = 500/1 ~ 200/1).

2a: White solid, 0.95 g, 1.05 mmol, 83%. M.p. 169–170 °C. ^{1}H NMR (DMSO-d_6, 300 MHz, 298 K) δ (ppm): 6.73–6.83 (m, 10H, Ar), 6.00 (t, J = 5.5 Hz, 1H, NH), 5.84 (t, J = 5.5 Hz, 1H, NH), 3.81 (t, J = 5.4 Hz, 2H, CH_2), 3.64–3.69 (m, 37H, CH_2, CH_3), 3.38–3.41 (m, 2H, CH_2), 2.86–2.93 (m, 2H, CH_2), 1.17–1.23 (m, 2H, CH_2), 1.03–1.12 (m, 6H, CH_2), 0.77 (t, J = 6.8 Hz, 3H, CH_3). ^{13}C NMR (DMSO-d_6, 75 MHz, 298 K) δ (ppm): 158.1, 150.01, 149.97, 149.87, 149.1, 127.8, 127.6, 127.5, 127.4, 114.4, 113.6, 113.3, 113.2, 113.1, 68.1, 55.4, 30.8, 29.9, 29.1, 29.0, 28.9, 28.8, 26.1, 21.9, 13.8. ESI-MS: *m/z* 907.4 $[M+H]^+$. HR-ESI-MS: *m/z* calcd for $[M+H]^+$ $C_{53}H_{67}N_2O_{11}$, 907.4739, found 907.4747.

2b: White solid, 0.99 g, 1.03 mmol, 82%. M.p. 163–164 °C. ^{1}H NMR (DMSO-d_6, 300 MHz, 298 K) δ (ppm): 6.75–6.81 (m, 10H, Ar), 5.80 (t, J = 5.5 Hz, 1H, NH), 5.64 (t, J = 5.5 Hz, 1H, NH), 3.82 (t, J = 5.2 Hz, 2H, CH_2), 3.66 (br, 37H, CH_2, CH_3), 3.03–3.09 (m, 2H, CH_2), 2.87–2.93 (m, 2H, CH_2), 1.70–1.79 (m, 2H, CH_2), 1.55–1.64 (m, 2H, CH_2), 1.19–1.28 (m, 2H, CH_2), 0.89–1.05 (m, 10H, CH_2), 0.69 (t, J = 6.9 Hz, 3H, CH_3). ^{13}C NMR (DMSO-d_6, 75 MHz, 298 K) δ (ppm): 158.1, 149.9, 149.2, 127.5, 127.4, 114.1, 113.14, 113.08, 67.6, 55.3, 55.2, 39.4, 39.1, 30.2, 27.0, 26.6, 21.7, 13.9. ESI-MS: *m/z* 963.5 $[M+H]^+$ (100%). HR-ESI-MS: *m/z* calcd for $[M+H]^+$ $C_{57}H_{75}N_2O_{11}$, 963.5371, found 963.5365.

1b: White solid, 1.08 g, 1.13 mmol, 90%. M.p. 107–108 °C. ^{1}H NMR (DMSO-d_6, 300 MHz, 298 K) δ (ppm): 8.43 (s, 1H, NH), 7.28 (d, J = 8.4 Hz, 2H, Ar), 7.04 (d, J = 8.4 Hz, 2H, Ar), 6.75–6.85 (m, 10H, Ar), 6.36 (t, J = 5.4 Hz, 1H, NH), 3.87 (t, J = 5.0 Hz, 2H, CH_2), 3.64–3.70 (m, 37H, CH_2, CH_3), 3.48–3.53 (m, 2H, CH_2), 2.48 (t, J = 7.9 Hz, 2H, CH_2), 1.44–1.54 (m, 2H, CH_2), 1.21–1.33 (m, 2H, CH_2), 0.87 (t, J = 7.3 Hz, 3H, CH_3). ^{13}C NMR (DMSO-d_6, 75 MHz, 298 K) δ (ppm): 155.3, 150.1, 150.0, 149.9, 149.1, 138.0, 135.0, 128.4, 127.8, 127.6, 127.5, 127.4, 117.7, 113.7, 113.30, 113.25, 67.7, 55.42, 55.39, 34.1, 33.2, 29.2, 29.0, 28.9, 28.8, 21.6, 13.7. ESI-MS: *m/z* 955.5 $[M+H]^+$ (100%). HR-ESI-MS: *m/z* calcd for $[M+H]^+$ $C_{57}H_{67}N_2O_{11}$, 955.4739,

found 955.4751.

8: To a solution of compound **3b** (1.04 g, 4.0 mmol) in dry DMF (15 mL) was added phthalimide (0.71 g, 4.8 mmol) and K_2CO_3 (0.83 g, 6.0 mmol) at room temperature. The reaction mixture was stirred overnight at 65 ^oC. After cooling, the solvent was removed under vacuum. Then water (40 mL) was added to the resulting mixture, and extracted with CH_2Cl_2 (2 × 40 mL). The organic layer was dried over anhydrous Na_2SO_4 and concentrated under reduced pressure. The crude product was purified by column chromatography (silica, CH_2Cl_2) to give **8** (1.24g, 3.8 mmol, 95%) as white solid. M.p. 65–66 ^oC. ^1H NMR (300 MHz, $CDCl_3$, 298 K) δ (ppm): 7.83–7.86(m, 2H, Ar), 7.70–7.73 (m, 2H, Ar), 6.81 (s, 4H, Ar), 3.94 (t, J = 5.9 Hz, 2H, CH_2), 3.77 (t, J = 6.8 Hz, 2H, CH_2), 3.76 (s, 3H, Me), 1.76–1.94 (m, 4H, CH_2). ^{13}C NMR (75 MHz, $CDCl_3$, 298 K) δ (ppm): 168.4, 153.8, 153.1, 133.9, 132.2, 123.2, 115.5, 114.6, 67.9, 55.7, 37.7, 26.8, 25.4. ESI-MS: *m/z* 348.1 $[M+Na]^+$ (100%). HR-ESI-MS: *m/z* calcd for $[M+Na]^+$ $C_{19}H_{19}NO_4Na$, 348.1206, found 348.1209.

9: Compound **8** (1.20 g, 3.69 mmol) was dissolved in THF (30 mL). The solution was heated to 65 ^oC and hydrazine monohydrate (85%, 2.1 mL, 36.9 mmol) was added. The reaction mixture was stirred overnight under argon atmosphere. After cooling, the solvent was removed. Then saturated aqueous Na_2CO_3 (80 mL) was added to the resulting mixture, and extracted with CH_2Cl_2 (2 × 80 mL). The organic layer was combined and dried over anhydrous Na_2SO_4 and concentrated under reduced pressure to give **9** (0.72 g, 3.68 mmol, 99%) as colorless oil. ^1H NMR ($CDCl_3$, 300 MHz, 298 K) δ (ppm): 6.83 (s, 4H, Ar), 3.93 (t, J = 6.5 Hz, 2H, CH_2), 3.77 (s, 3H, Me), 2.77 (t, J = 6.9 Hz, 2H, CH_2), 1.76–1.85 (m, 2H, CH_2), 1.57–1.66 (m, 2H, CH_2). ^{13}C NMR ($CDCl_3$, 75 MHz, 298 K) δ (ppm): 153.8, 153.2, 115.5, 114.7, 68.5, 55.8, 42.0, 30.4, 26.8. ESI-MS: *m/z* 196.1 $[M+H]^+$ (100%). HR-ESI-MS: *m/z* calcd for $[M+H]^+$ $C_{11}H_{18}NO_2$, 196.1332, found 196.1347.

1c: To a solution of compound **9** (0.70 g, 3.58 mmol) in dry CH_2Cl_2 (50 mL) was

added 1-octyl isocyanate (0.67 g, 4.30 mmol) under argon atmosphere. The reaction mixture was stirred overnight at room temperature. After the solvent was removed under vacuum, the residue was washed by diethyl ether to give **1c** (1.10 g, 3.14 mmol, 88%) as white solid. M.p. 114–115 ^{o}C. ^{1}H NMR (DMSO-d_6, 300 MHz, 298 K) δ (ppm): 6.84 (s, 4H, Ar), 5.78 (t, J = 5.8 Hz, 1H, NH), 5.73 (t, J = 5.8 Hz, 1H, NH), 3.88 (t, J = 6.4 Hz, 2H, CH_2), 3.69 (s, 3H, Me), 2.98–3.05 (m, 2H, CH_2), 2.92–2.98 (m, 2H, CH_2), 1.61–1.70 (m, 2H, CH_2), 1.43–1.52 (m, 2H, CH_2), 1.30–1.36 (m, 2H, CH_2), 1.24 (br, 10H, CH_2), 0.85 (t, J = 6.6 Hz, 3H, CH_3). ^{13}C NMR (DMSO-d_6, 75 MHz, 298 K) δ (ppm): 158.1, 153.2, 152.6, 115.3, 114.5, 67.7, 55.3, 31.2, 30.0, 28.7, 26.7, 26.4, 26.2, 22.1, 13.9. ESI-MS: *m/z* 373.3 $[M+Na]^+$ (100%). HR-ESI-MS: *m/z* calcd for $[M+H]^+$ $C_{20}H_{35}N_2O_3$, 351.2642, found 351.2647.

^{1}H NMR and ^{13}C NMR spectra of the compounds synthesized

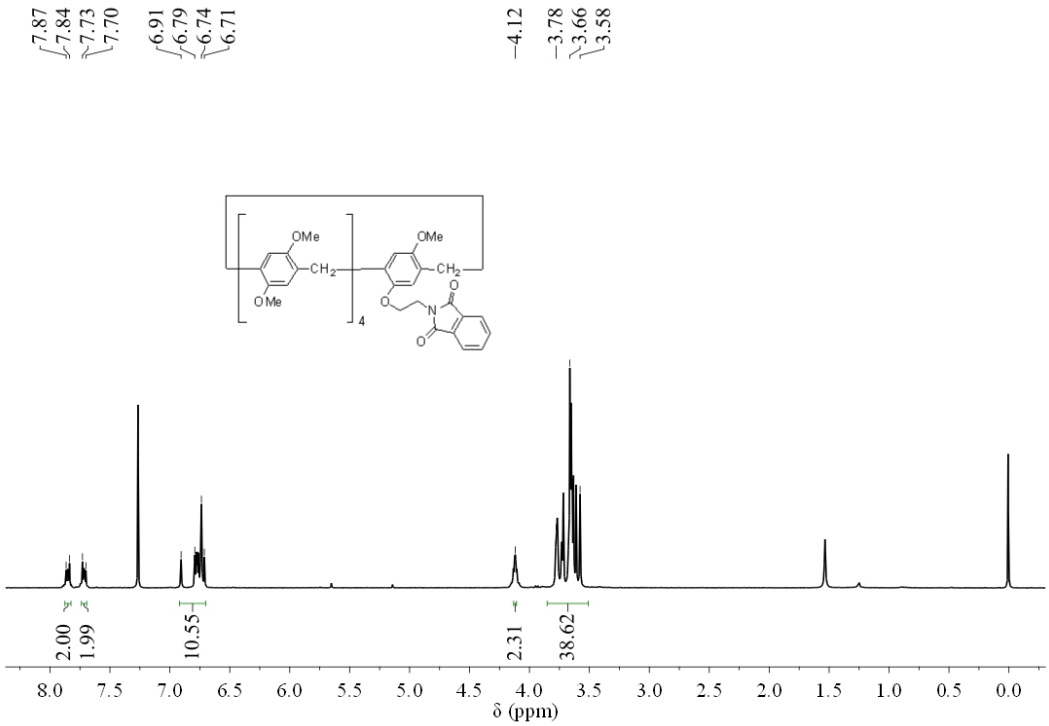

Figure S1. ^{1}H NMR spectrum (300 MHz, $CDCl_3$, 298 K) of **6a**.

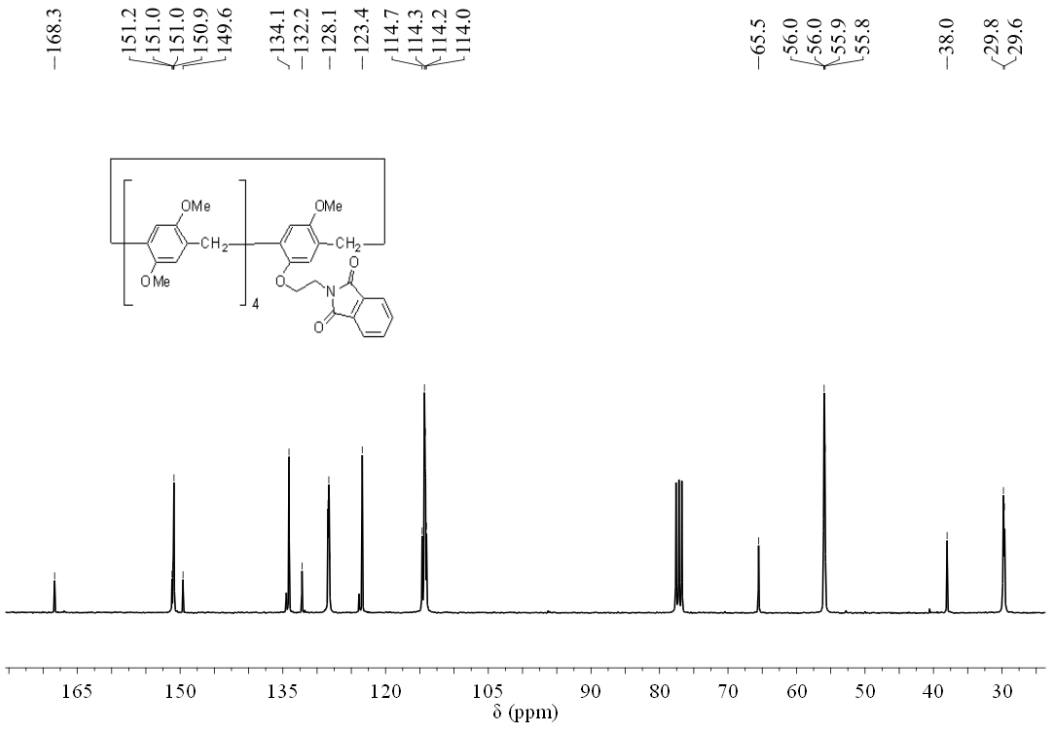

Fig. S2 ^{13}C NMR spectrum (75 MHz, $CDCl_3$, 298 K) of **6a**.

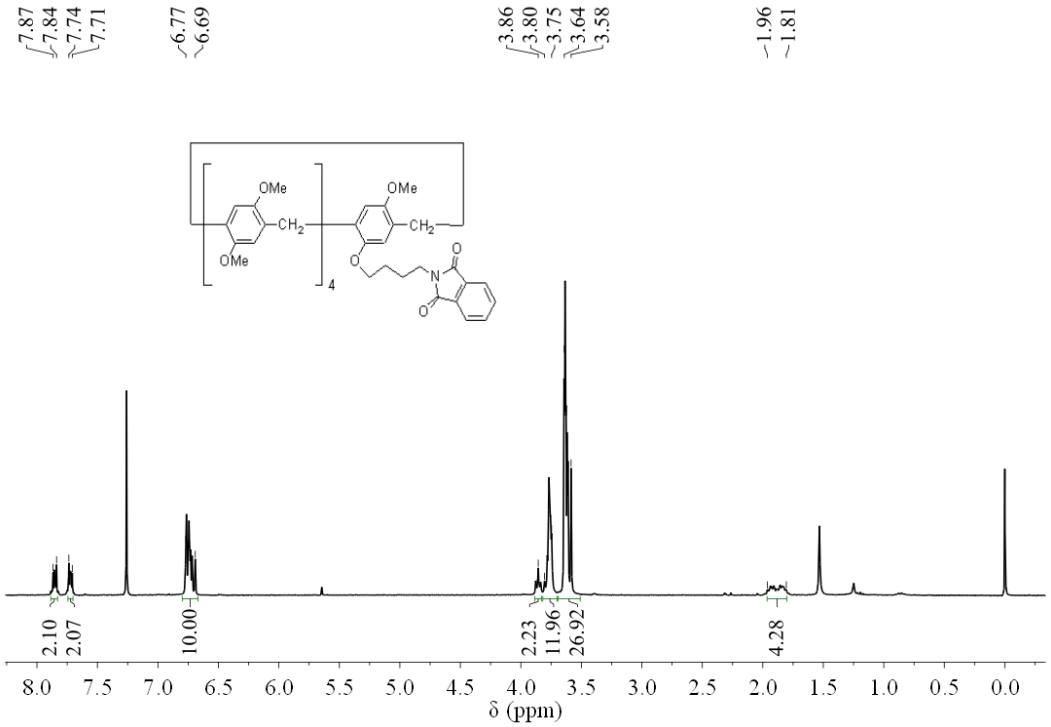

Fig. S3 ^{1}H NMR spectrum (300 MHz, $CDCl_3$, 298 K) of **6b**.

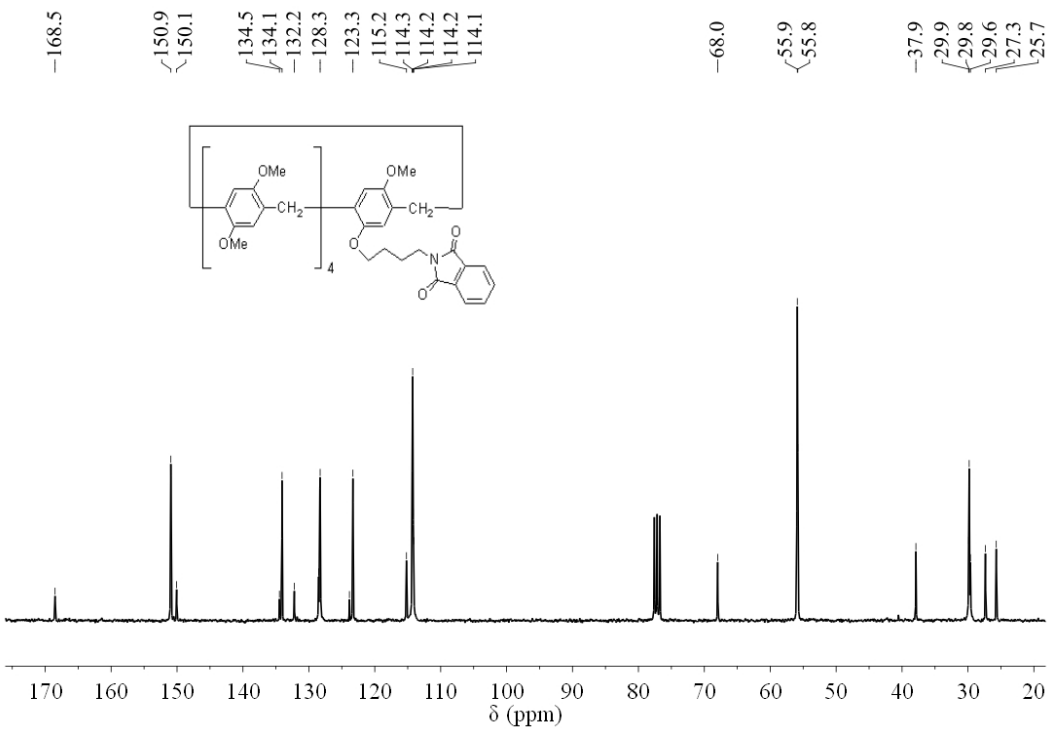

Fig. S4 ^{13}C NMR spectrum (75 MHz, $CDCl_3$, 298 K) of **6b**.

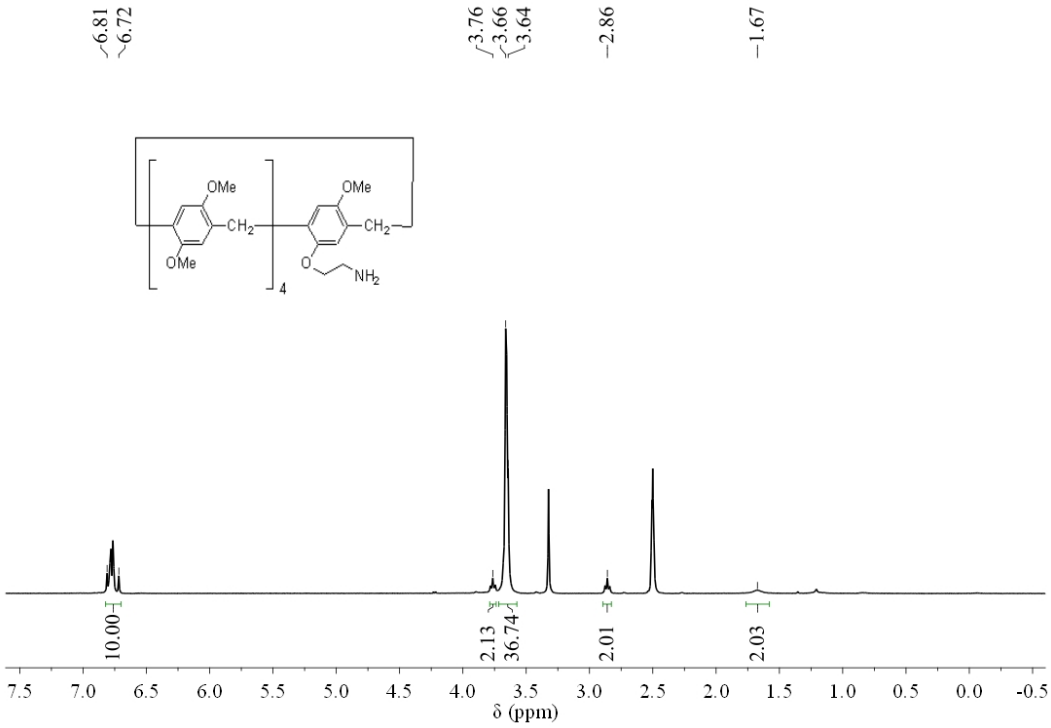

Fig. S5 ^{1}H NMR spectrum (300 MHz, DMSO-d_6, 298 K) of **7a**.

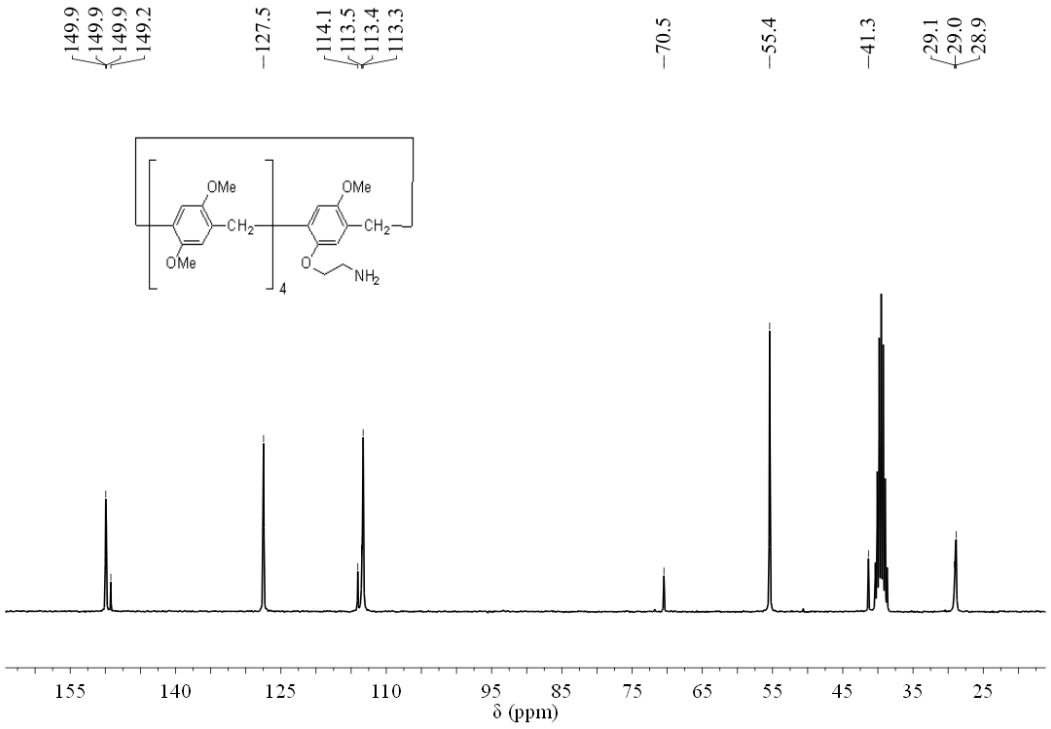

Fig. S6 ^{13}C NMR spectrum (75 MHz, DMSO-d_6, 298 K) of **7a**.

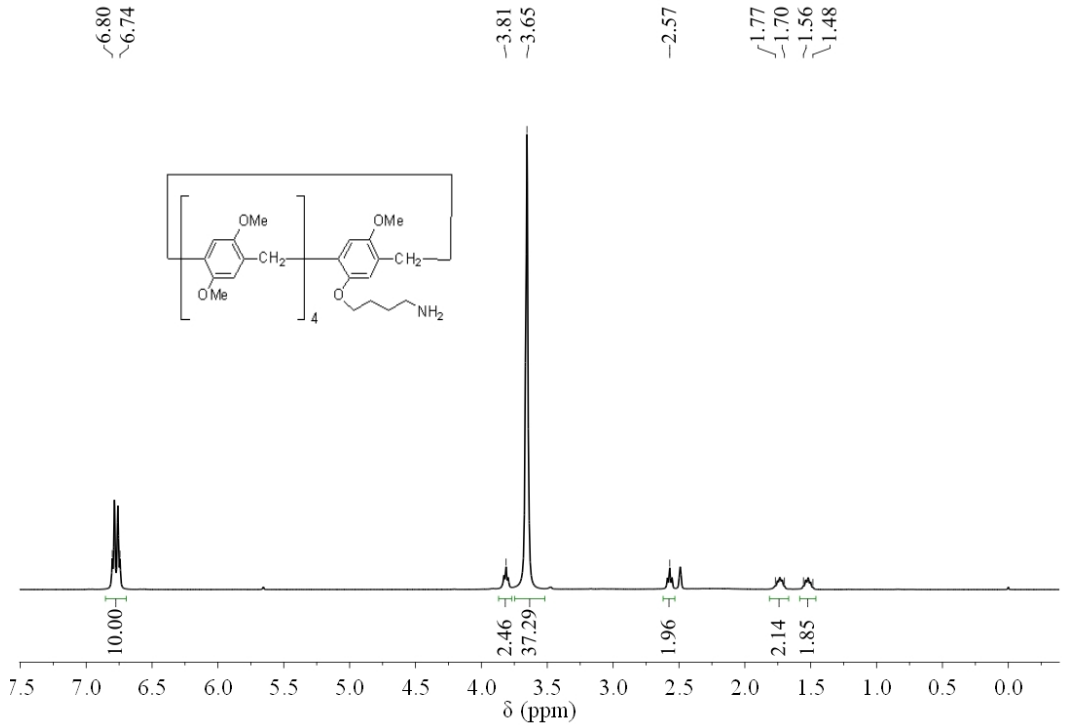

Fig. S7 ^{1}H NMR spectrum (400 MHz, DMSO-d_6, 298 K) of **7b**.

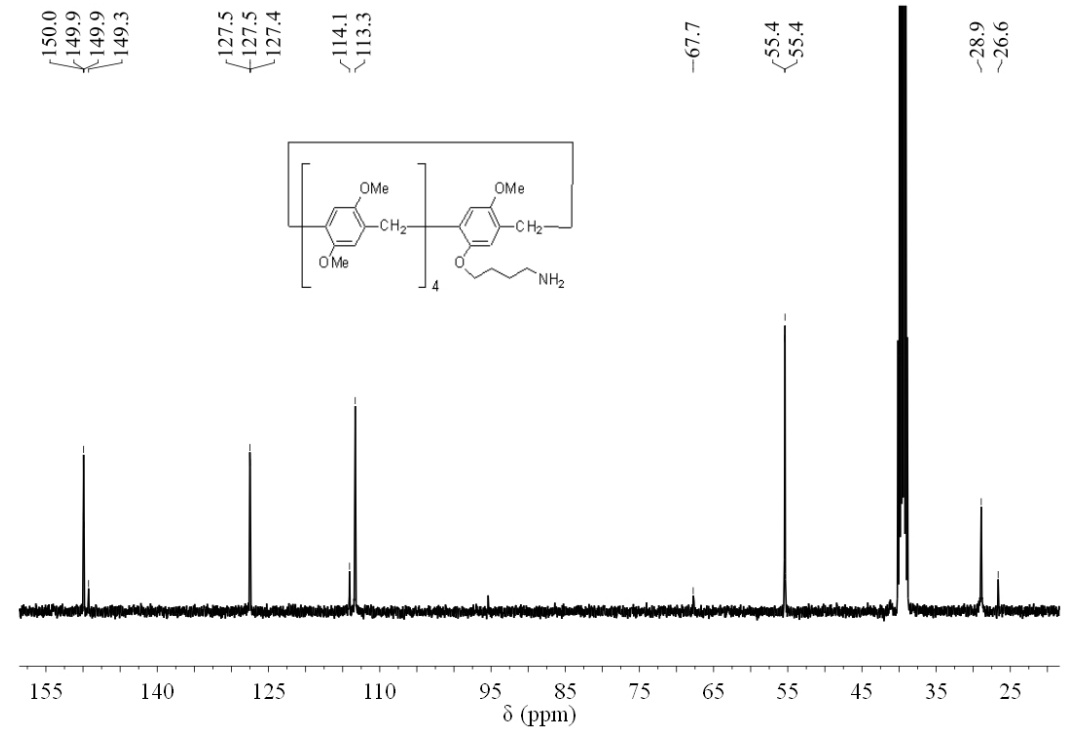

Fig. S8 ^{13}C NMR spectrum (100 MHz, DMSO-d_6, 298 K) of **7b**.

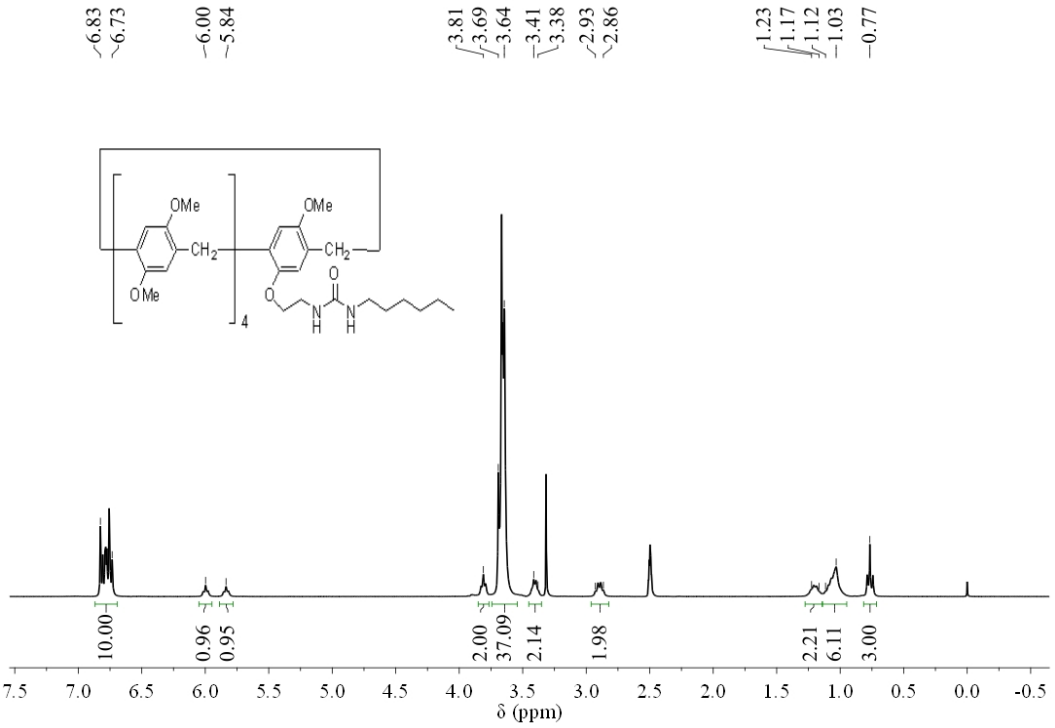

Fig. S9 ^{1}H NMR spectrum (300 MHz, DMSO-d_6, 298 K) of **2a**.

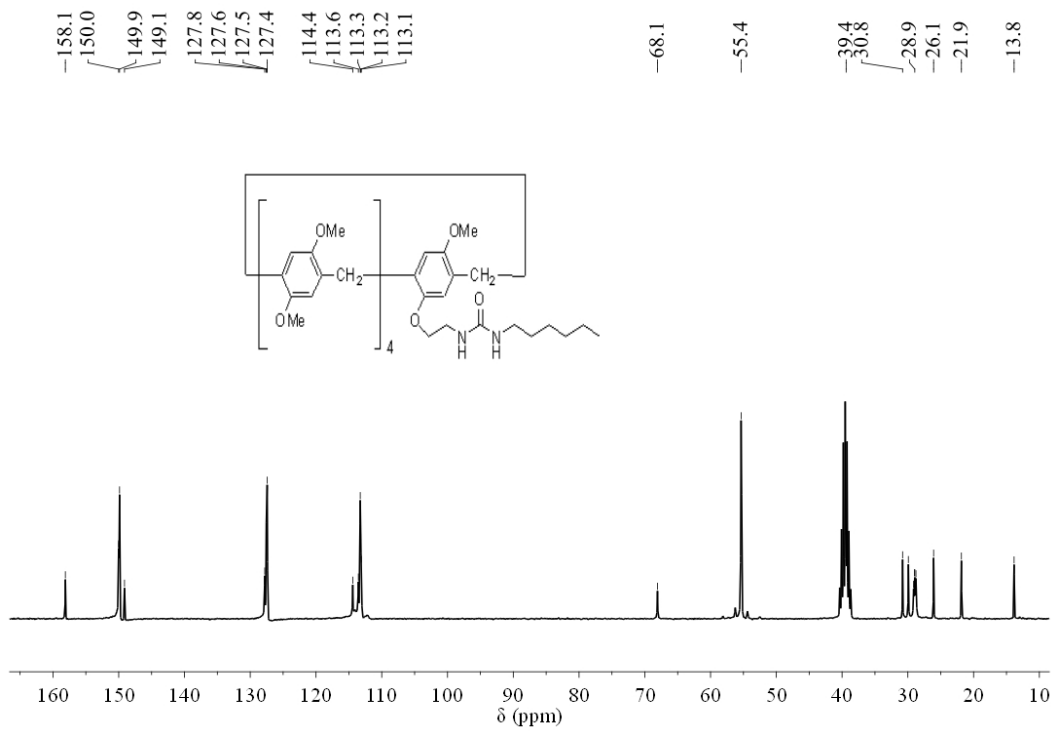

Fig. S10 ^{13}C NMR spectrum (75 MHz, DMSO-d_6, 298 K) of **2a**.

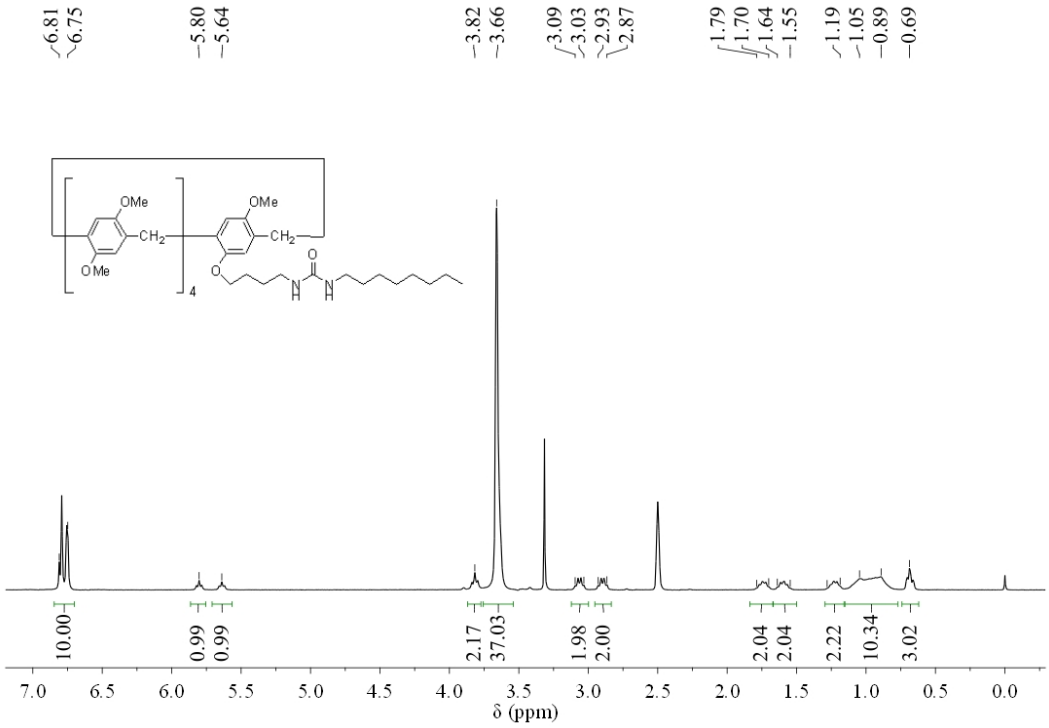

Fig. S11 ^{1}H NMR spectrum (300 MHz, DMSO-d_6, 298 K) of **2b**.

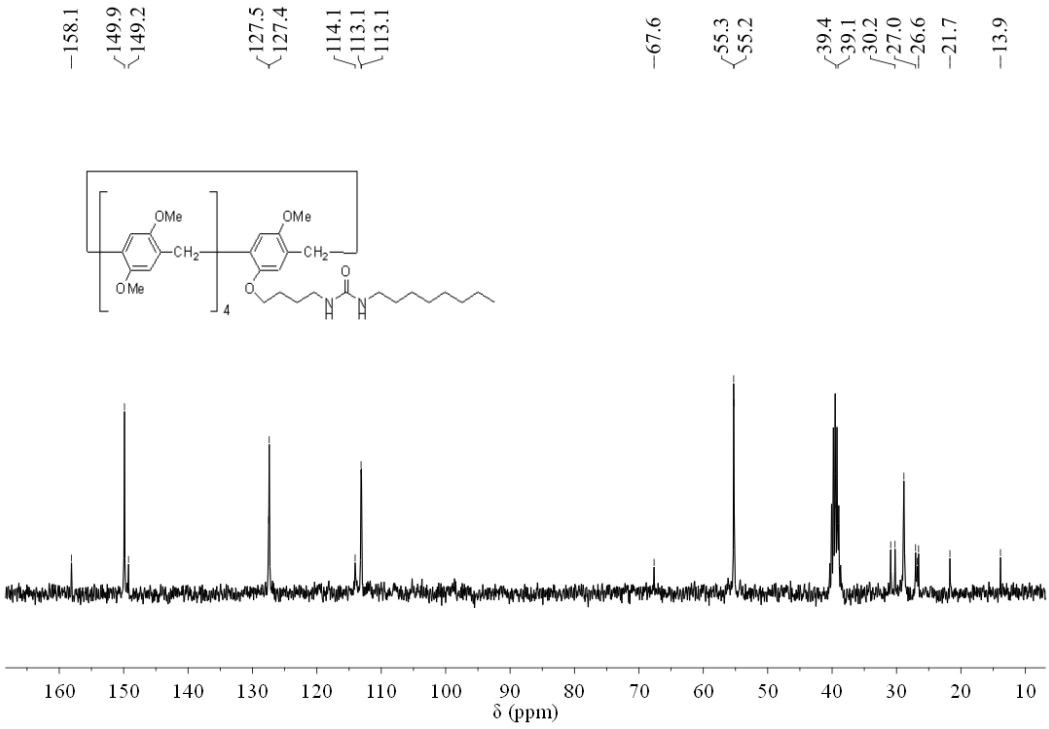

Fig. S12 ^{13}C NMR spectrum (75 MHz, DMSO-d_6, 298 K) of **2b**.

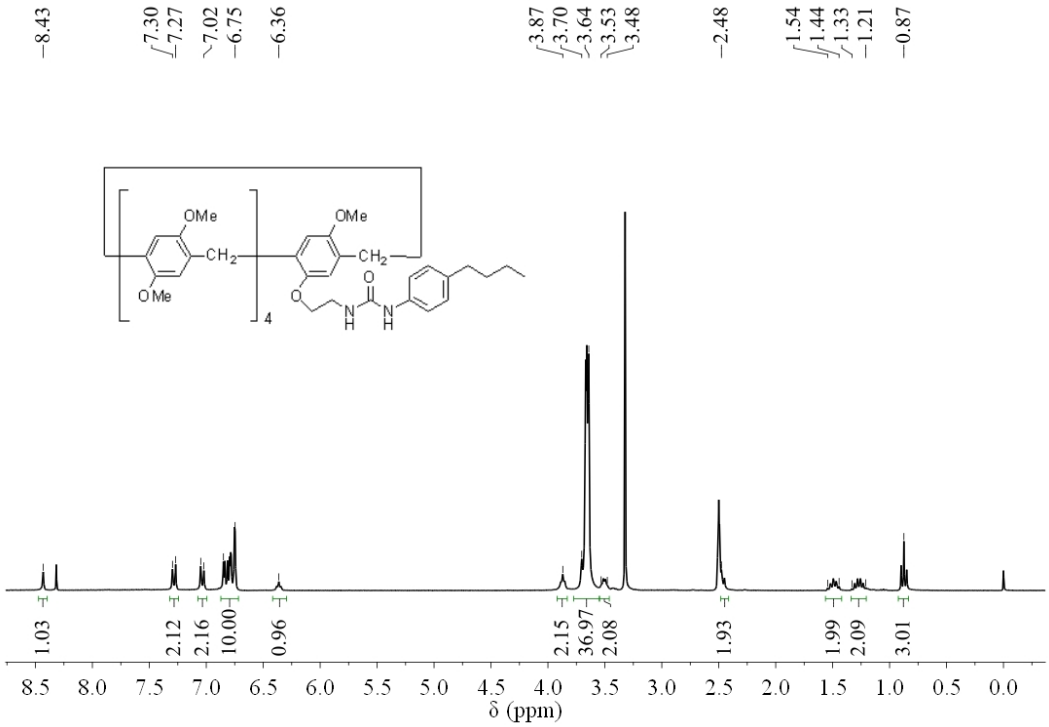

Fig. S13 ^{1}H NMR spectrum (300 MHz, DMSO-d_6, 298 K) of **1b**.

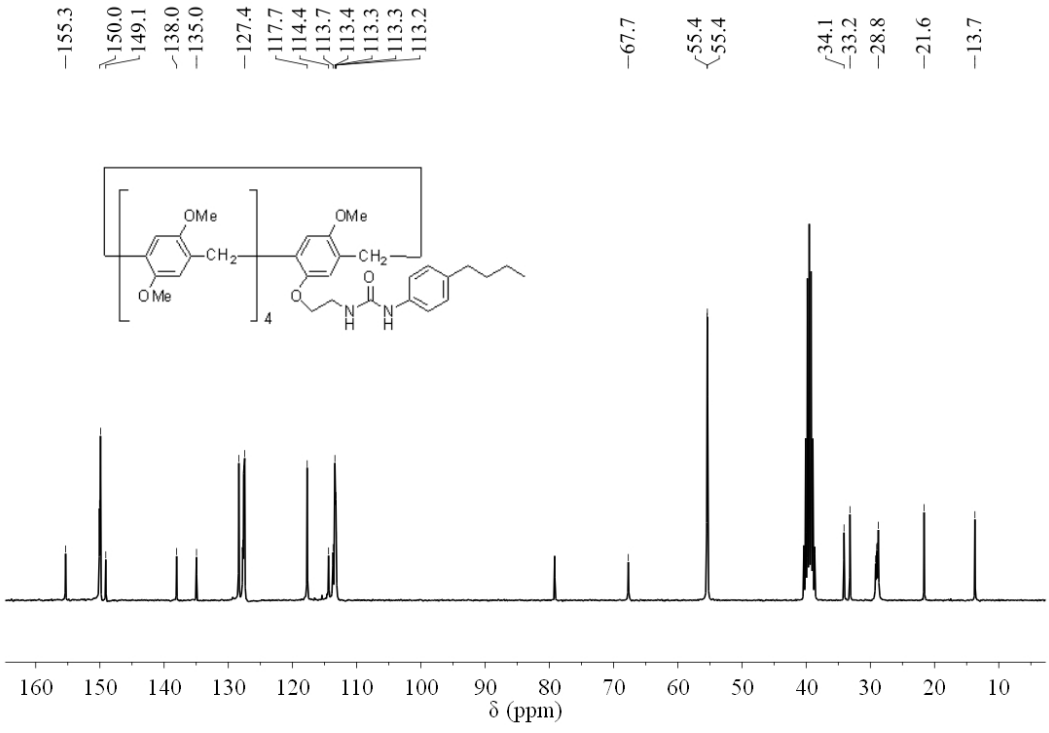

Fig. S14 ^{13}C NMR spectrum (75 MHz, DMSO-d_6, 298 K) of **1b**.

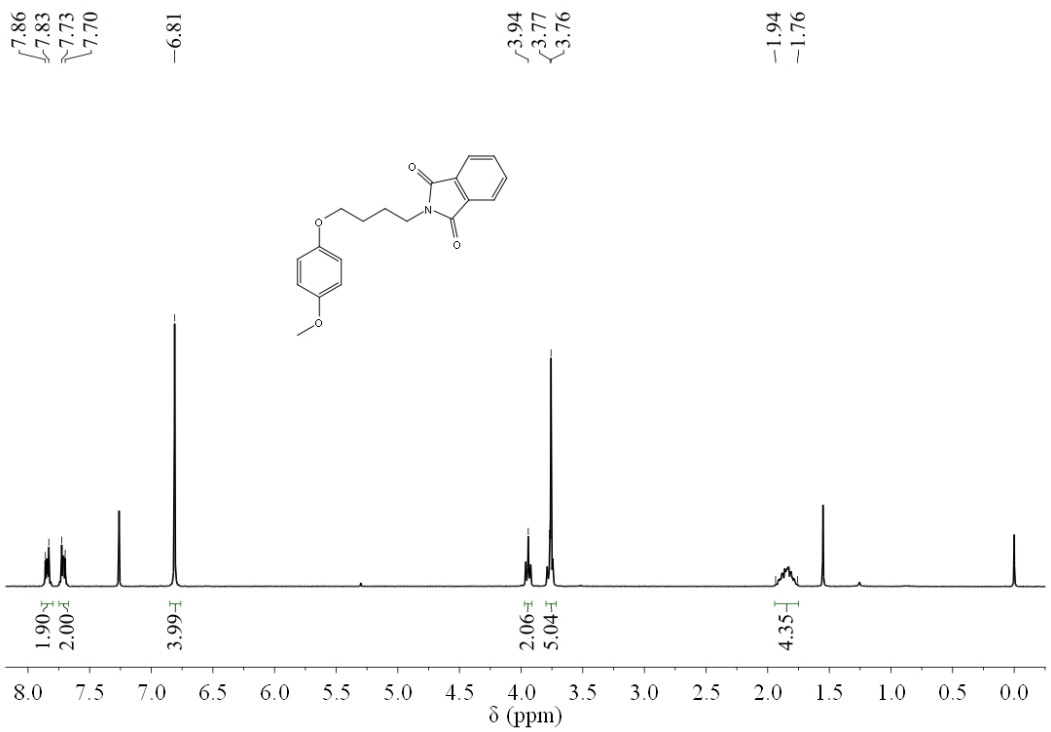

Fig. S15 ^{1}H NMR spectrum (300 MHz, $CDCl_3$, 298 K) of **8**.

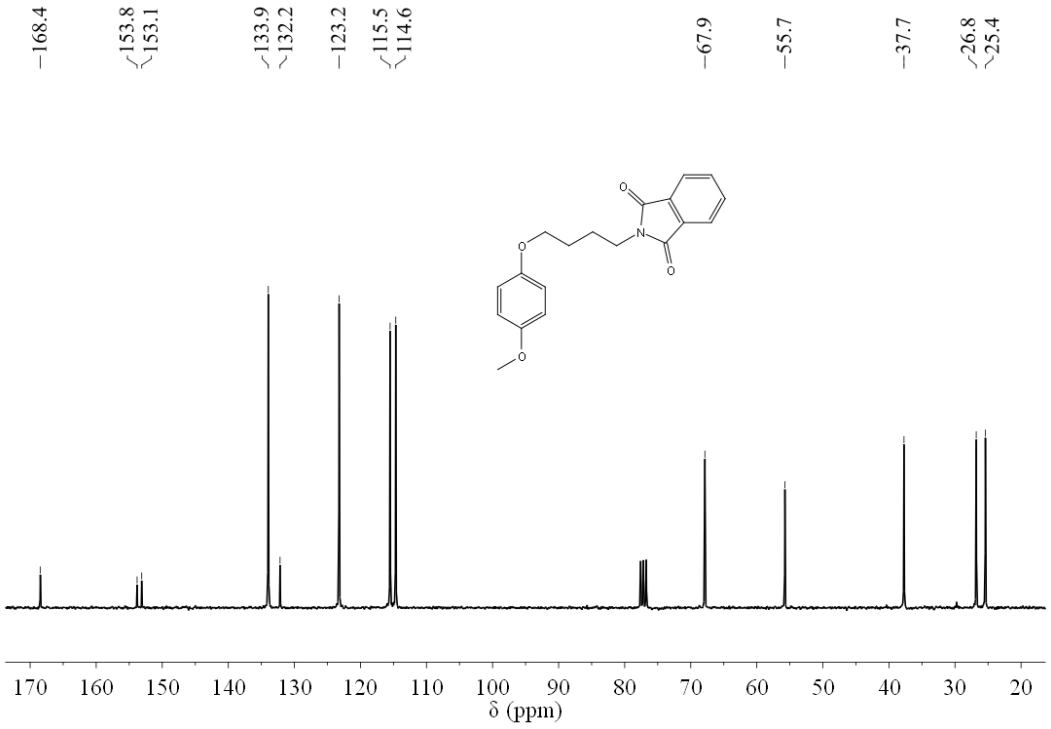

Fig. S16 ^{13}C NMR spectrum (75 MHz, $CDCl_3$, 298 K) of **8**.

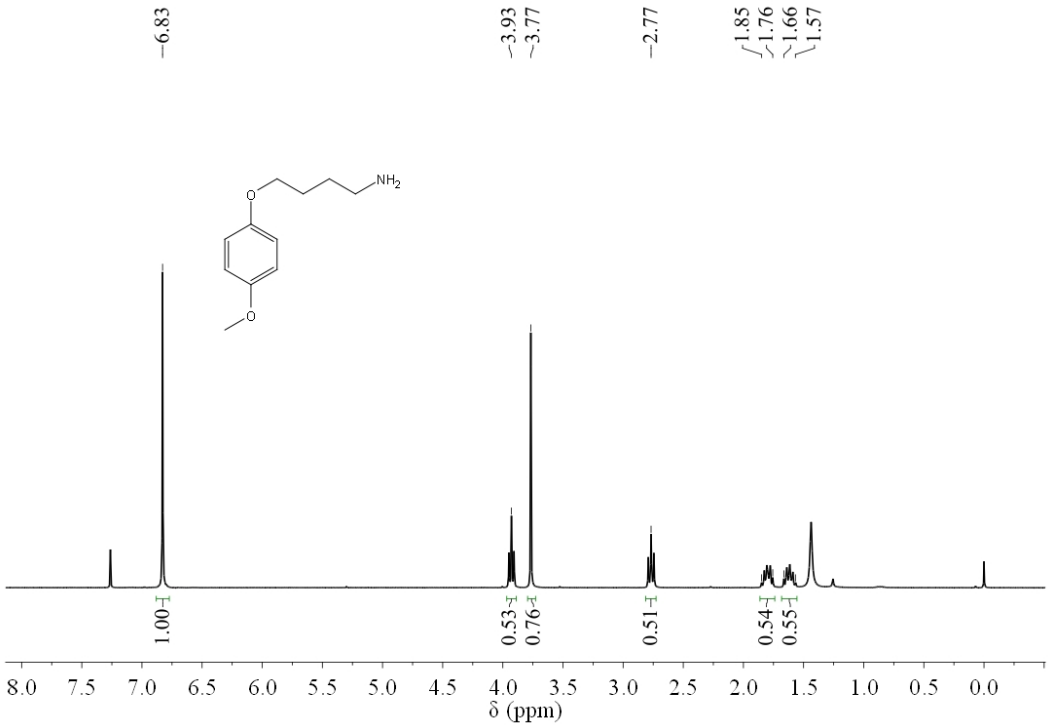

Fig. S17 ^{1}H NMR spectrum (300 MHz, $CDCl_3$, 298 K) of **9**.

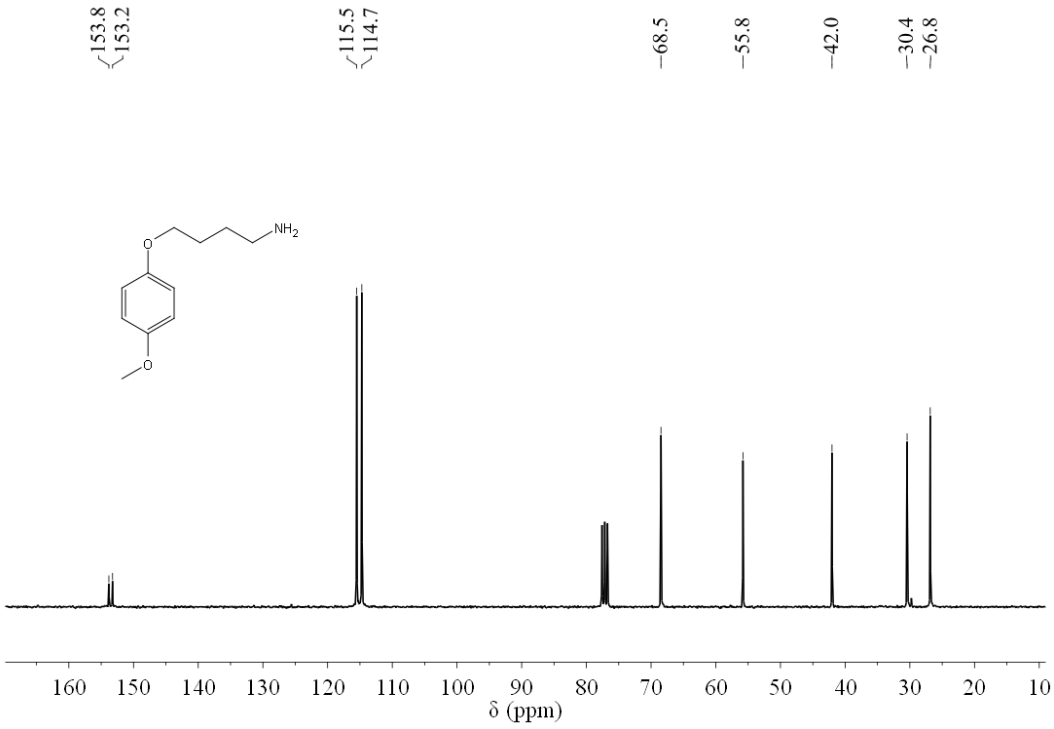

Fig. S18 ^{13}C NMR spectrum (75 MHz, $CDCl_3$, 298 K) of **9**.

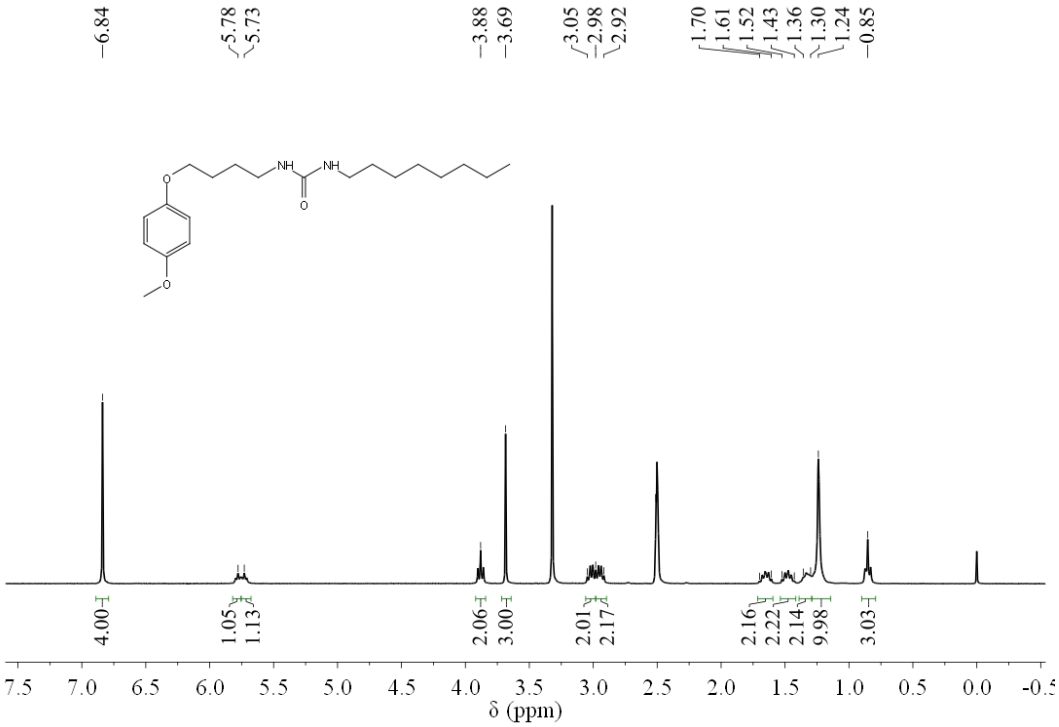

Fig. S19 ^{1}H NMR spectrum (300 MHz, DMSO-d_6, 298 K) of **1c**.

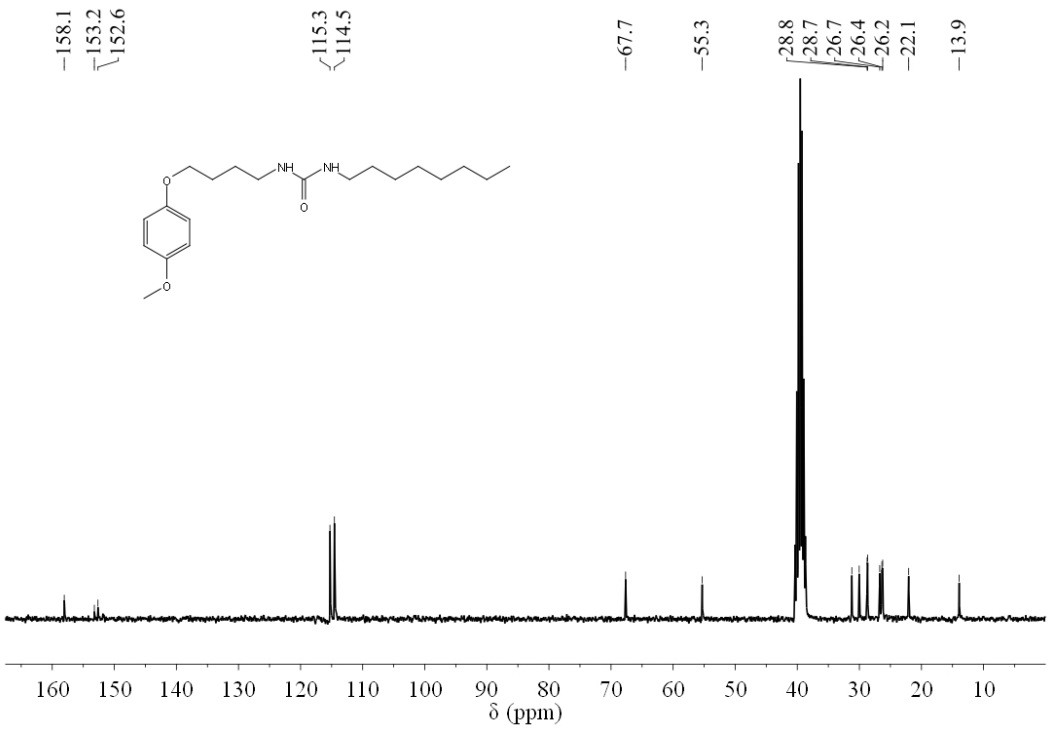

Fig. S20 ^{13}C NMR spectrum (75 MHz, DMSO-d_6, 298 K) of **1c**.

*[1]H NMR spectra of **1c**, **2b**, **2a**, and **1b** in different solvents*

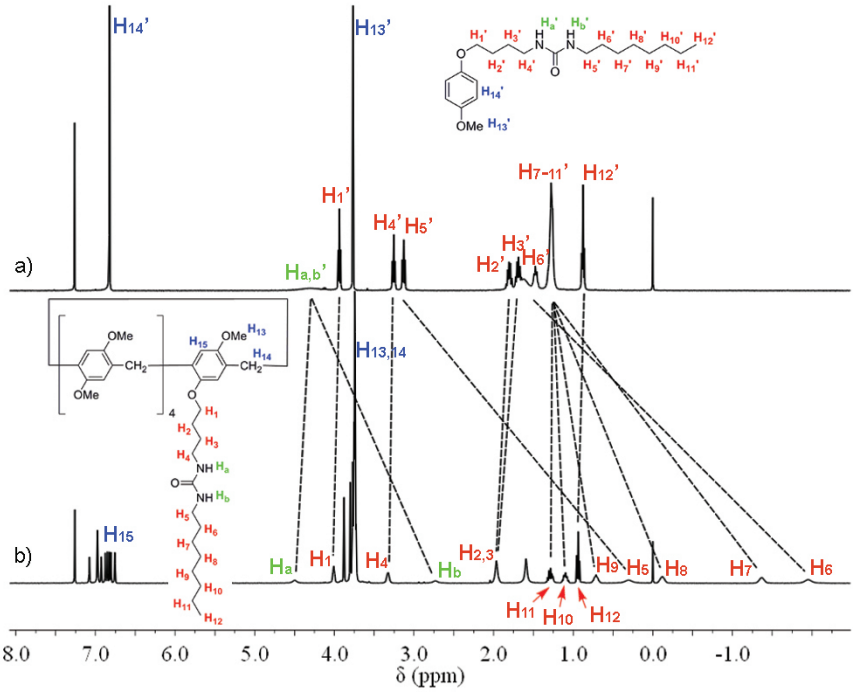

Fig. S21 [1]H NMR spectra (400 MHz, 298 K) of (a) **1c** (8 mM) and (b) **2b** (8 mM) in $CDCl_3$.

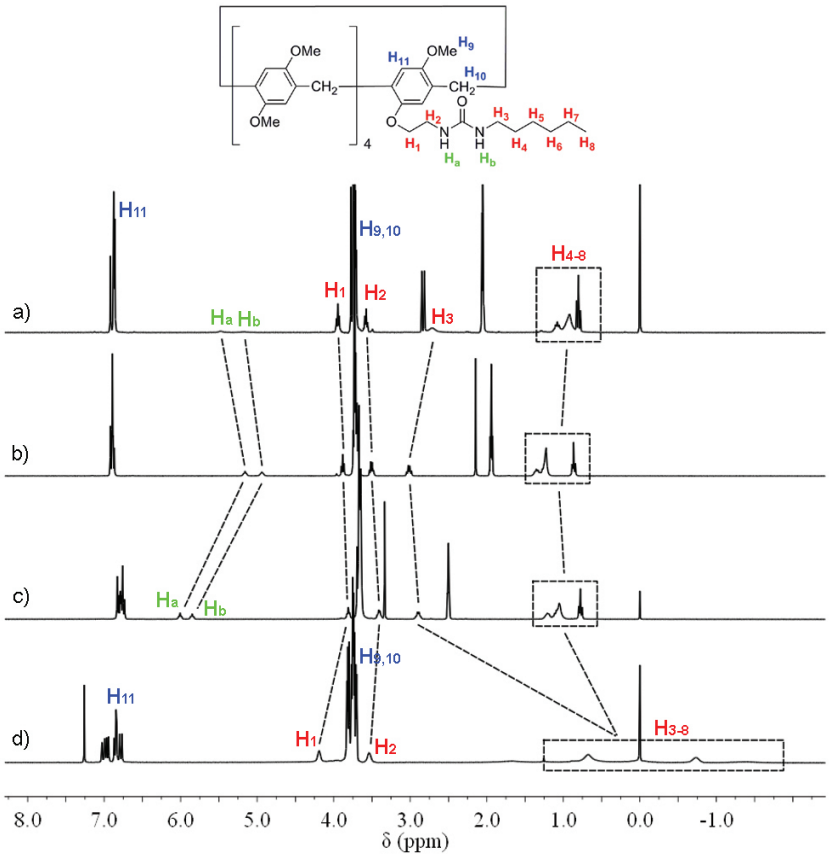

Fig. S22 [1]H NMR spectra (300 MHz, 298 K) of **2a** (8 mM) in (a) acetone-d_6, (b) CD_3CN, (c) DMSO-d_6, and (d) $CDCl_3$.

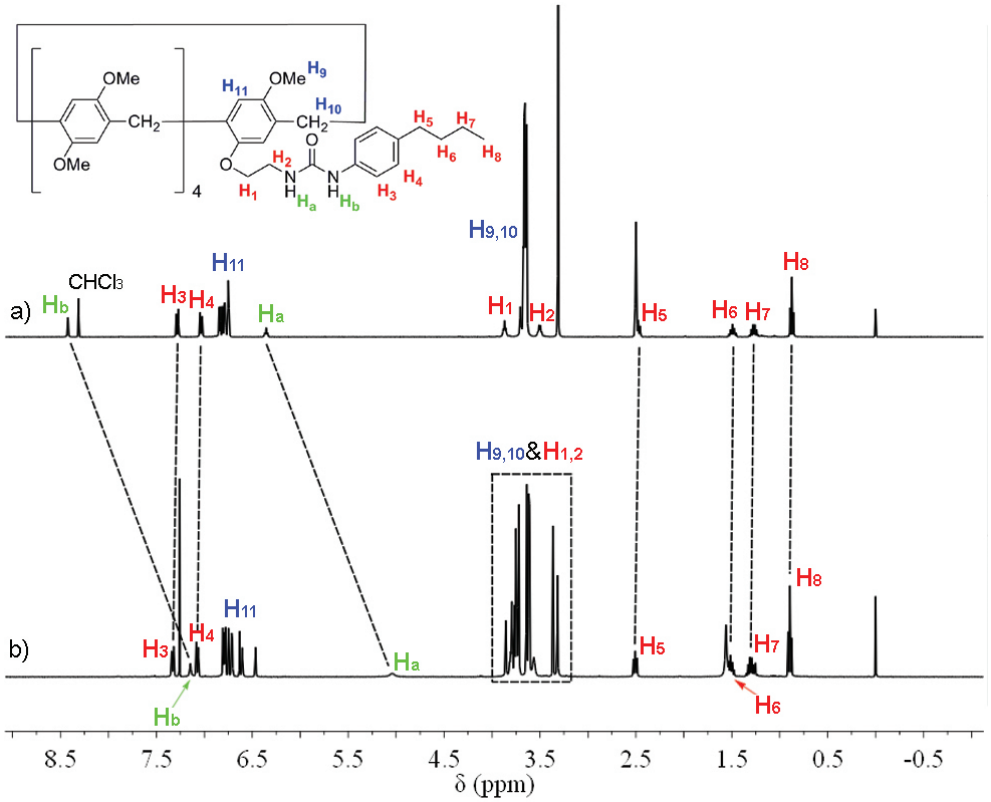

Fig. S23 ^{1}H NMR spectra (400 MHz, 298 K) of **1b** (8 mM) in (a) DMSO-d_6 and (b) $CDCl_3$.

*COSY spectra of **2a** and **2b***

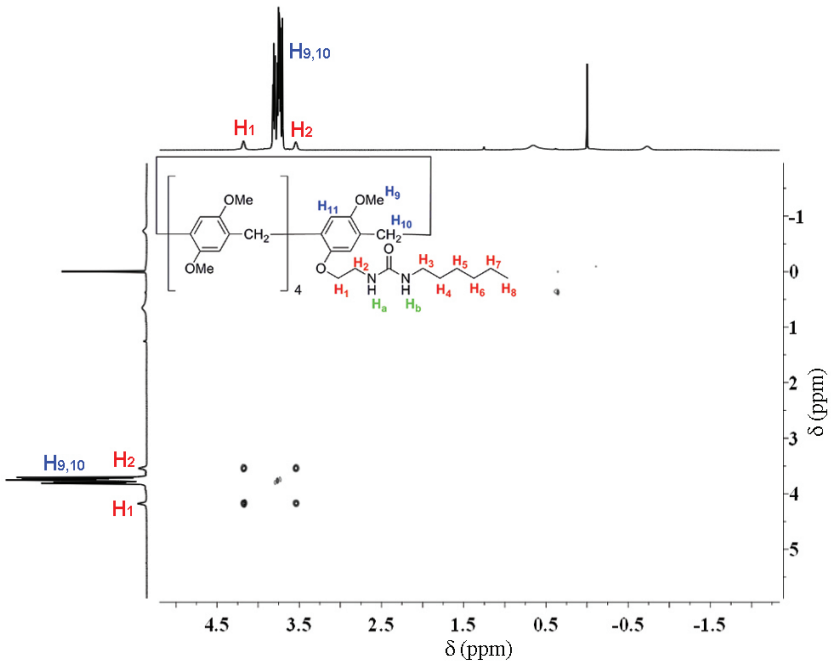

Fig. S24 Partial 2D COSY spectrum (400 MHz, $CDCl_3$, 298 K) of **2a** (20 mM). The peaks for H_3–H_8 were so broad that the correlation signals could not be observed, making it difficult to assign the peaks accurately.

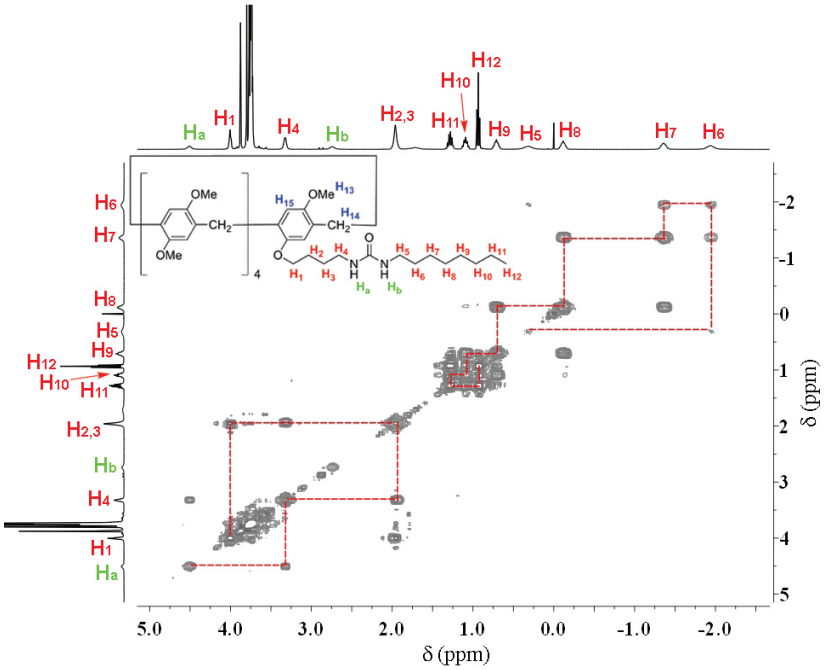

Fig. S25 Partial 2D COSY spectrum (400 MHz, $CDCl_3$, 298 K) of **2b** (25 mM).

*NOESY spectra of **2a** and **2b***

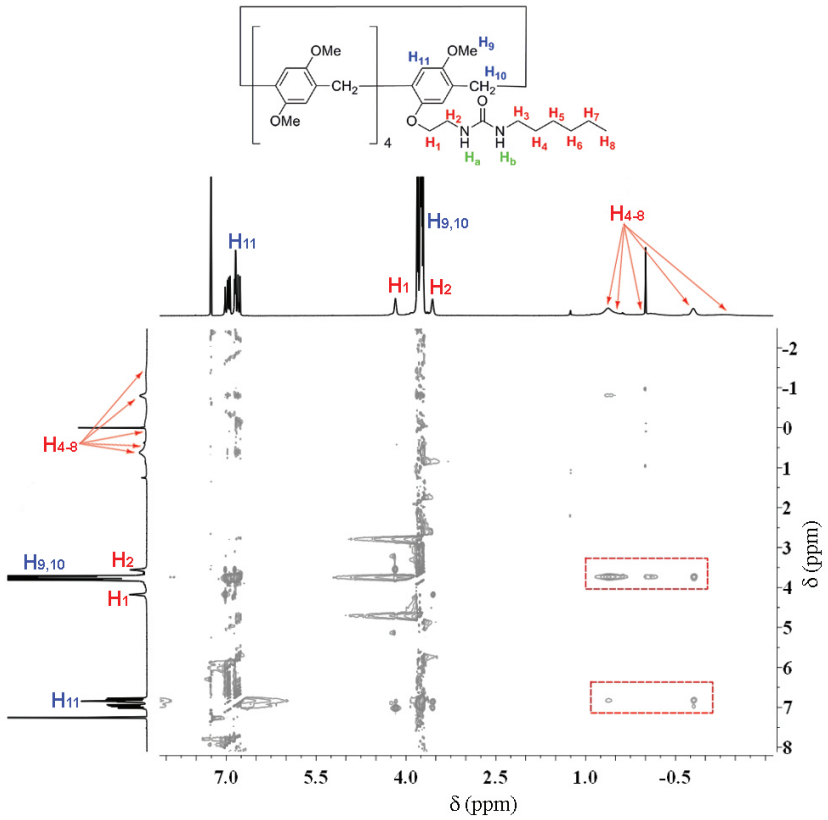

Fig. S26 Partial 2D NOESY spectrum (400 MHz, $CDCl_3$, 298 K) of **2a** (25 mM) with a mixing time of 300 ms.

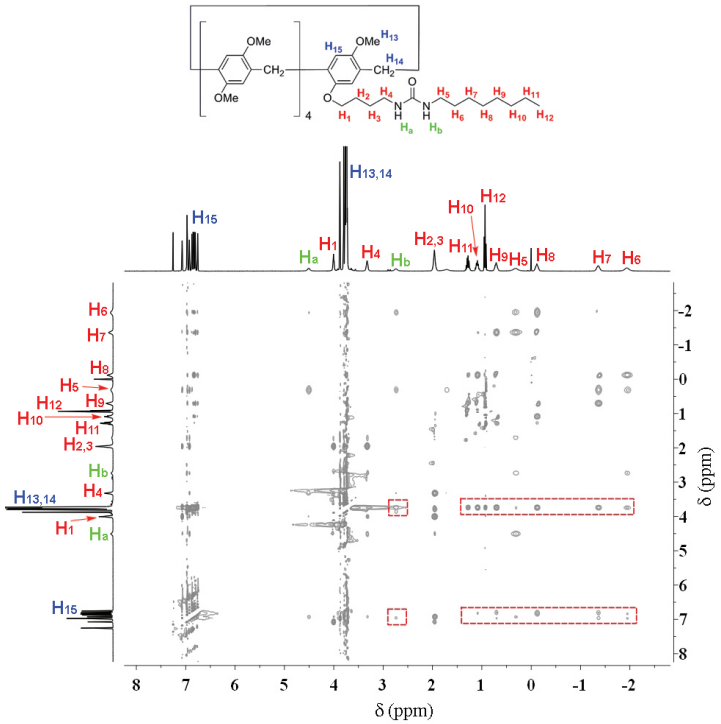

Fig. S27 Partial 2D NOESY spectrum (400 MHz, $CDCl_3$, 298 K) of **2b** (25 mM) with a mixing time of 300 ms.

*^{1}H NMR spectra of **2a**, **2b**, and **1c** at different concentrations*

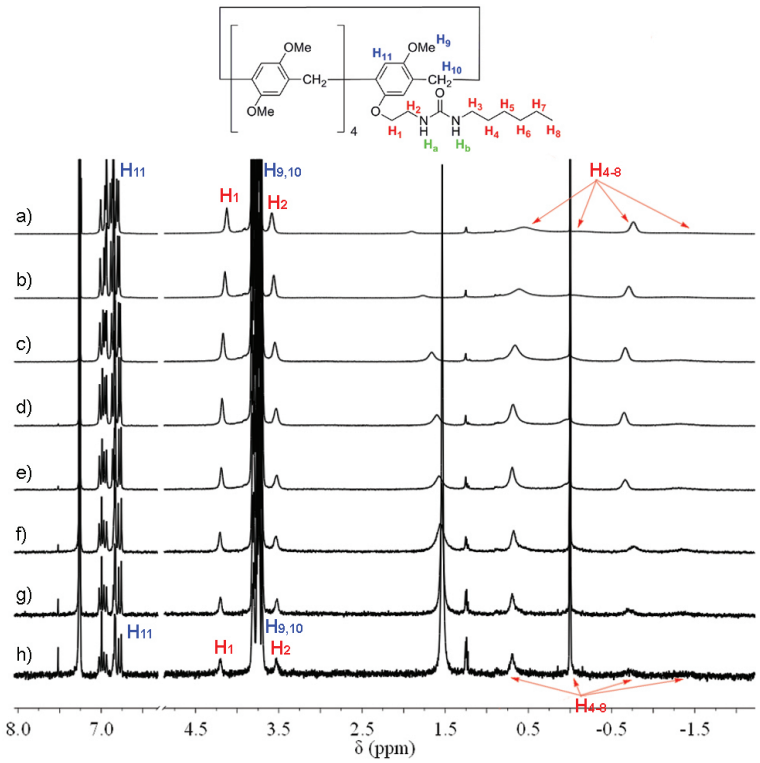

Fig. S28 ^{1}H NMR spectra (400 MHz, $CDCl_3$, 298 K) of **2a** at different concentrations: (a) 100 mM, (b) 50 mM, (c) 20 mM, (d) 10 mM, (e) 5 mM, (f) 2 mM, (g) 1 mM, and (h) 0.5 mM.

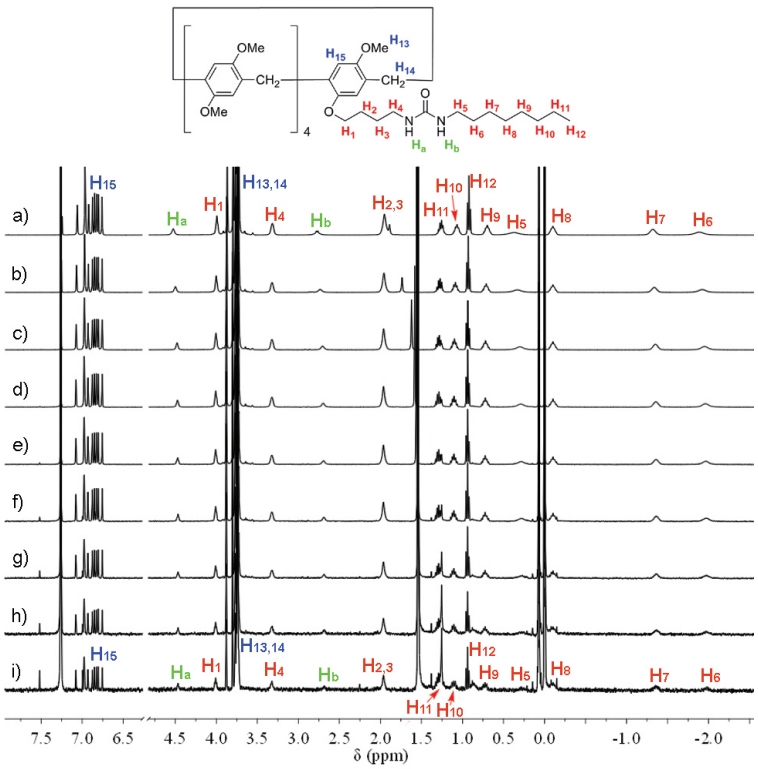

Fig. S29 ^{1}H NMR spectra (400 MHz, $CDCl_3$, 298 K) of **2b** at different concentrations: (a) 100 mM, (b) 50 mM, (c) 20 mM, (d) 10 mM, (e) 5 mM, (f) 2 mM, (g) 1 mM, (h) 0.5 mM, and (i) 0.3 mM.

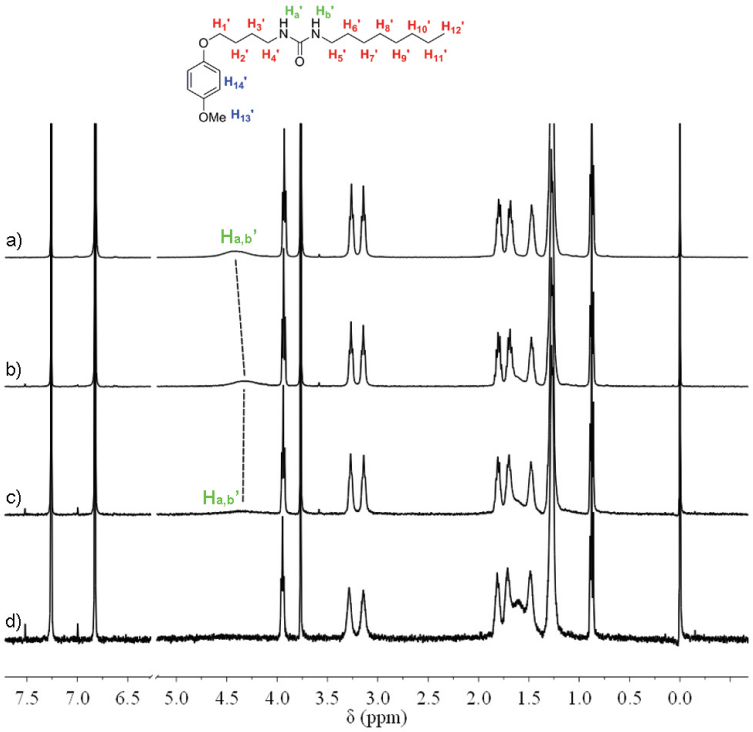

Fig. S30 ^{1}H NMR spectra (400 MHz, $CDCl_3$, 298 K) of **1c** at different concentrations: (a) 30 mM, (b) 12 mM, (c) 5 mM, and (d) 2 mM. Notice that the signals of the urea protons shifted downfield as the concentration of **1c** increased.

*ESI-MS spectra of **2a** and **2b***

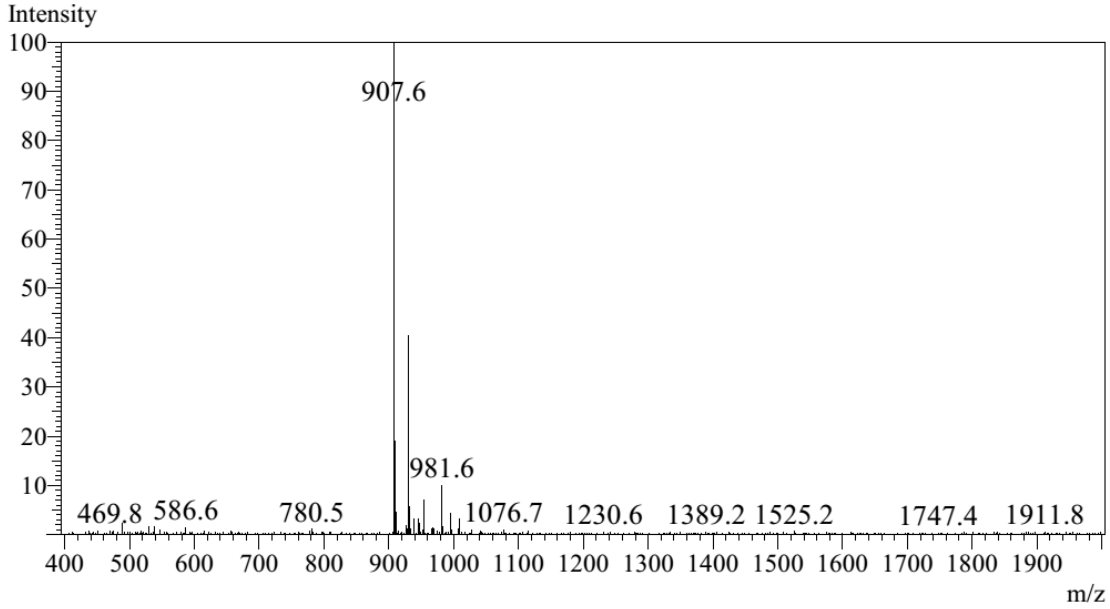

Fig. S31. ESI-MS spectrum of **2a** in acetonitrile in the positive ion mode. The peak at *m/z* = 907.6 was corresponding to the monomer [**2a**+H]$^+$, while no peak for the dimer could be found.

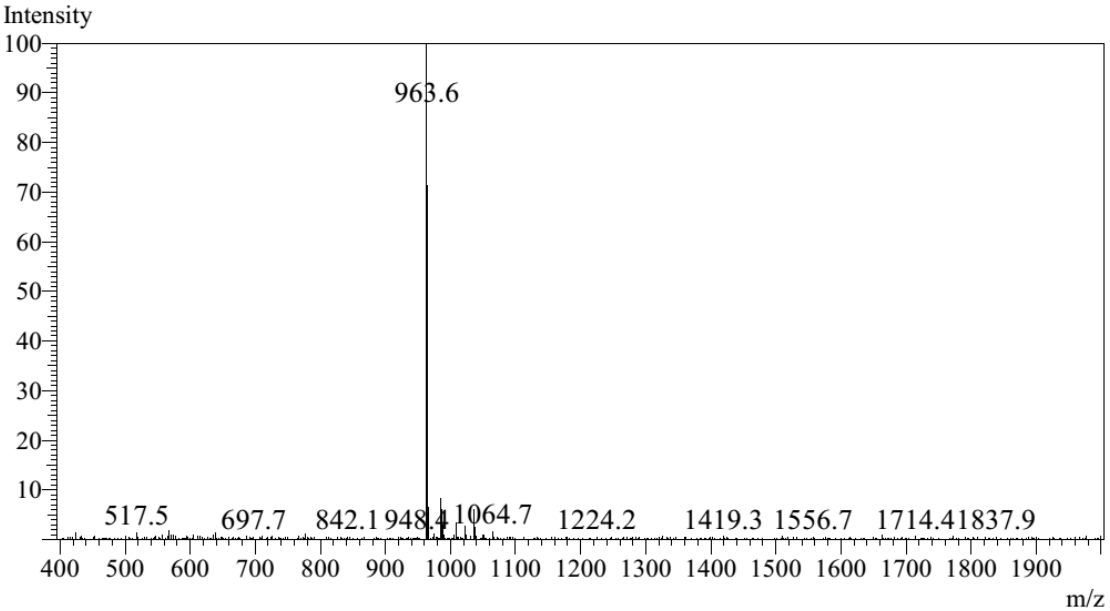

Fig. S32. ESI-MS spectrum of **2b** in acetonitrile in the positive ion mode. The peak at *m/z* = 963.6 was corresponding to the monomer [**2b**+H]$^+$, while no peak for the dimer could be found.

DOSY experiments

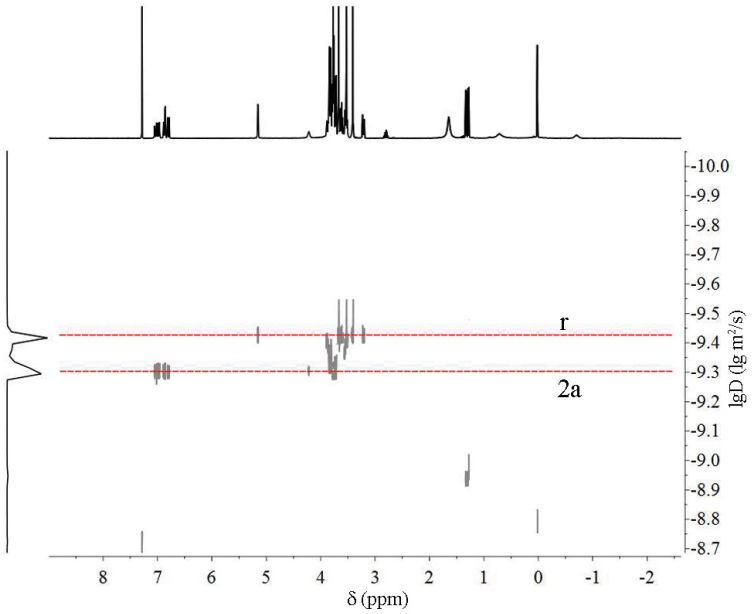

Fig. S33 DOSY spectrum (400 MHz, $CDCl_3$, 291 K) of **2a** (M = 907 g/mol, 2M = 1814 g/mol) at a concentration of 4 mM with the addition of heptakis(2,3,6-tri-*O*-methyl)-*β*-cyclodextrin (M = 1429 g/mol, labeled as "r") as the internal reference. Notice that only one set of signals of **2a** could be observed from the DOSY spectrum ($D = 5.01\times10^{-10}$ $m^2\cdot s^{-1}$).

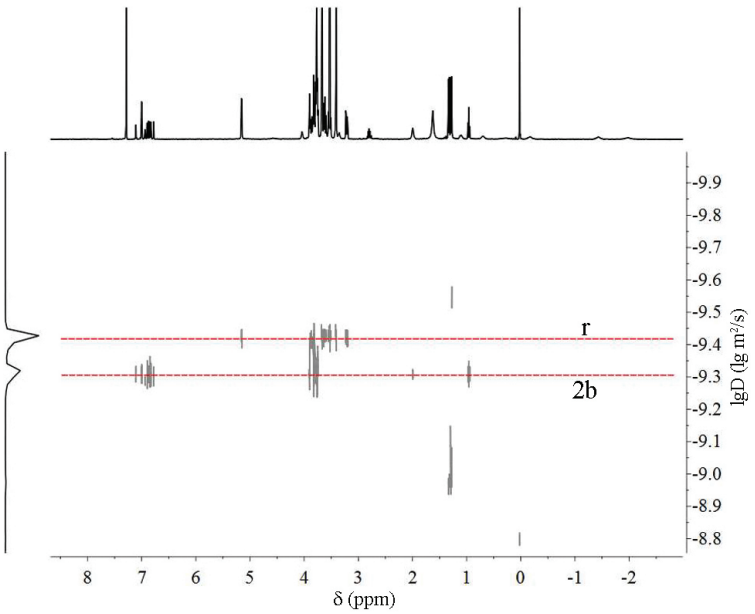

Fig. S34 DOSY spectrum (400 MHz, $CDCl_3$, 291 K) of **2b** (M = 963 g/mol, 2M = 1926 g/mol) at a concentration of 4 mM with the addition of heptakis(2,3,6-tri-*O*-methyl)-*β*-cyclodextrin (M = 1429 g/mol, labeled as "r") as the internal reference. Notice that only one set of signals of **2b** could be observed from the DOSY spectrum. ($D = 4.93\times10^{-10}$ $m^2\cdot s^{-1}$).

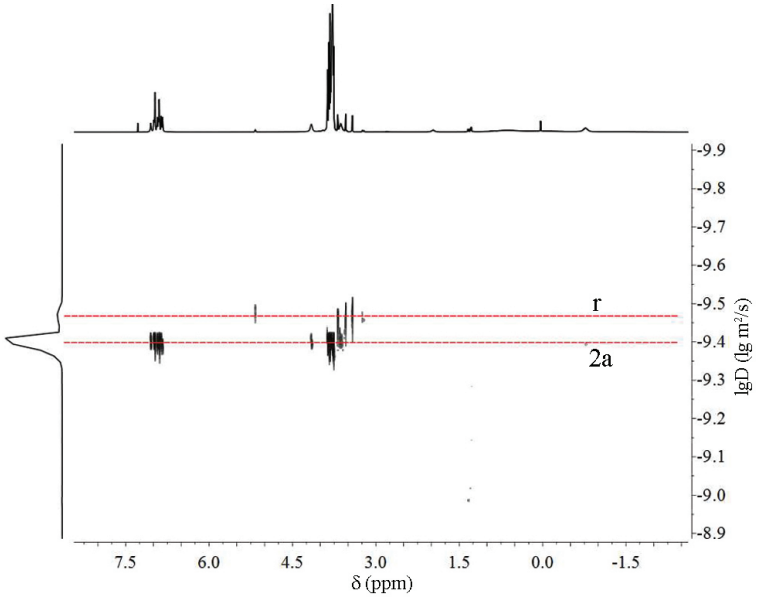

Fig. S35 DOSY spectrum (400 MHz, $CDCl_3$, 291 K) of **2a** (M = 907 g/mol, 2M = 1814 g/mol) at a concentration of 100 mM with the addition of heptakis(2,3,6-tri-*O*-methyl)-*β*-cyclodextrin (M = 1429 g/mol, labeled as "r") as the internal reference. Notice that only one set of signals of **2a** could be observed from the DOSY spectrum ($D = 3.96\times10^{-10}$ $m^2\cdot s^{-1}$).

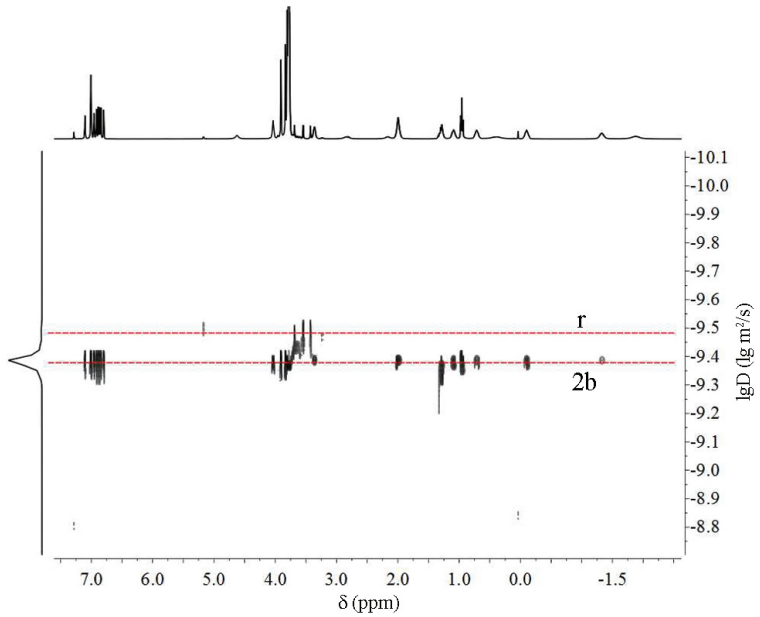

Fig. S36 DOSY spectrum (400 MHz, $CDCl_3$, 291 K) of **2b** (M = 963 g/mol, 2M = 1926 g/mol) at a concentration of 100 mM with the addition of heptakis(2,3,6-tri-*O*-methyl)-*β*-cyclodextrin (M = 1429 g/mol, labeled as "r") as the internal reference. Notice that only one set of signals of **2b** could be observed from the DOSY spectrum. ($D = 4.09\times10^{-10}$ $m^2\cdot s^{-1}$).

Considering the fact that the viscosity of the solution increased with the rising of solution concentration, the diffusion coefficient of **2a** and **2b** did not change much as the concentration increased from 4 mM to 100 mM, which was in agreement with the

results of variable concentration ^{1}H NMR spectroscopy (Fig. S28–S29).

The hydrodynamic radii of **2a** and **2b** in $CDCl_3$ were calculated by the Stokes-Einstein relation (Equation 1).

$$r_s = \frac{kT}{6\pi\eta D} \qquad \text{Equation 1}$$

where D is the diffusion coefficient (obtained from Fig. S33–S34), k is the Boltzmann constant (1.3807×10^{-23} $m^2\cdot kg\cdot s^{-2}\cdot K^{-1}$), T is the temperature in Kelvin (291 K), η is the viscosity of the solution (chloroform 5.37×10^{-4} $kg\cdot m^{-1}\cdot s^{-1}$), and r_s is the radius of the molecular sphere. The calculation results were listed in Table S1. And from the crystal structure of **2a**, the hydrodynamic radius of the [c2]daisy chain was obtained ca. 12.18 Å (Fig. S37), which was much larger than the calculated hydrodynamic radii of **2a** and **2b** in $CDCl_3$ solutions (Table S1). The comparison also confirmed the formation of pseudo[1]rotaxanes of **2a** and **2b** in $CDCl_3$.

Table S1 The hydrodynamic radii calculated from the DOSY experiments

Samples	**2a**	**2b**
lg$D$ (lg $m^2\cdot s^{-1}$)	–9.3003	–9.3068
D (10^{-10} $m^2\cdot s^{-1}$)	5.01	4.93
r_s (Å)	7.92	8.05

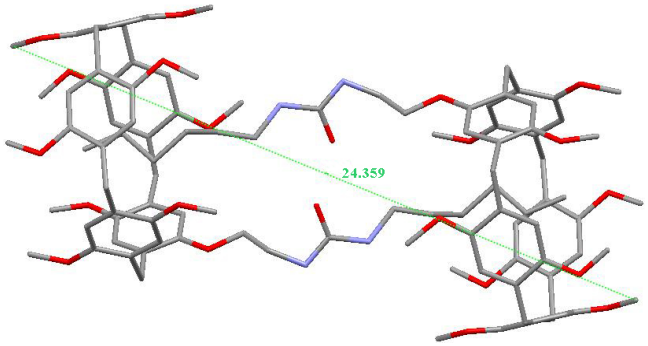

Fig. S37 Crystal structure of **2a**. The hydrodynamic radius of the [c2]daisy chain was 12.18 Å, which was half of the length of the green dotted line. For details, see Fig. S48.

Moreover, we also used 1,4-dimethoxypillar[5]arene[S5] (**DMP5**, Scheme S2) as the internal reference in the DOSY experiments considering the structure similarity between **2a**, **2b** and **DMP5**. As expected, the diffusion coefficients of **2a** and **2b** were close to that of **DMP5**. These results also convinced the formation of pseudo[1]rotaxanes of **2a** and **2b** in $CDCl_3$.

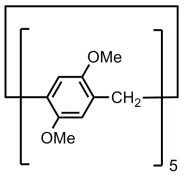

Scheme S2 The structure of **DMP5**.

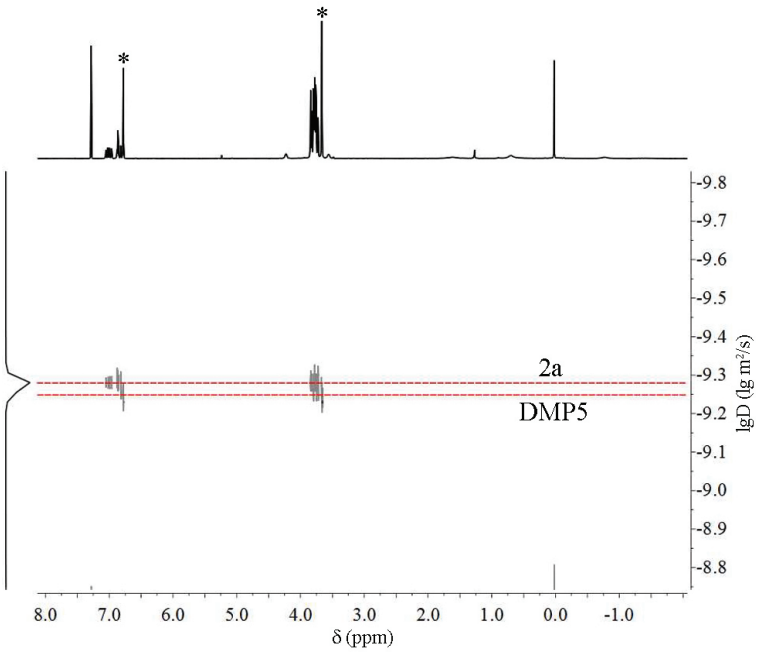

Fig. S38 DOSY spectrum (400 MHz, $CDCl_3$, 291 K) of **2a** (M = 907 g/mol) at a concentration of 4 mM with the addition of **DMP5** (M = 751 g/mol) as the internal reference. The diffusion coefficients of **2a** and **DMP5** were 5.25×10^{-10} $m^2\cdot s^{-1}$ and 5.71×10^{-10} $m^2\cdot s^{-1}$, respectively. Asterisk = **DMP5**.

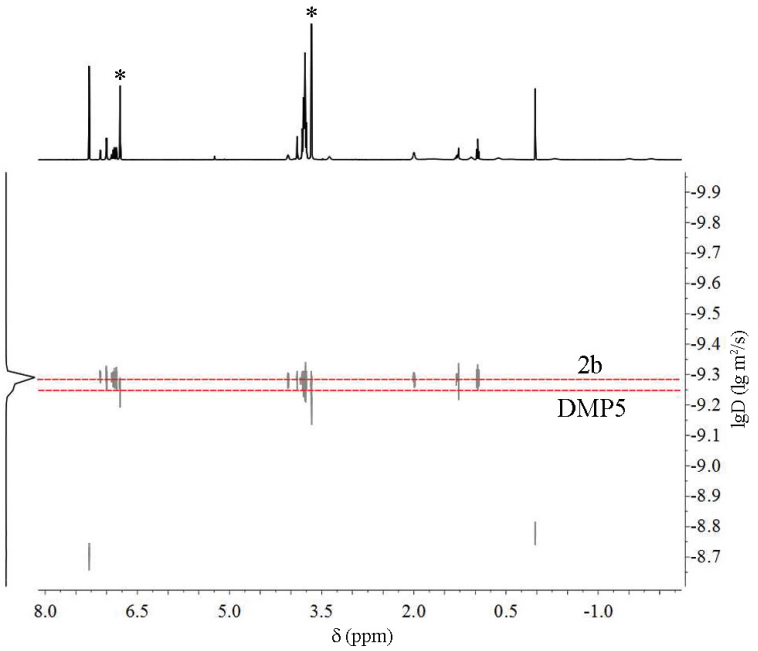

Fig. S39 DOSY spectrum (400 MHz, $CDCl_3$, 291 K) of **2b** (M = 963 g/mol) at a concentration of 4 mM with the addition of **DMP5** (M = 751 g/mol) as the internal reference. The diffusion coefficients of **2b** and **DMP5** were 5.13×10^{-10} $m^2\cdot s^{-1}$ and 5.66×10^{-10} $m^2\cdot s^{-1}$, respectively. Asterisk = **DMP5**.

*FTIR spectra of **2a** and **2b** in $CHCl_3$*

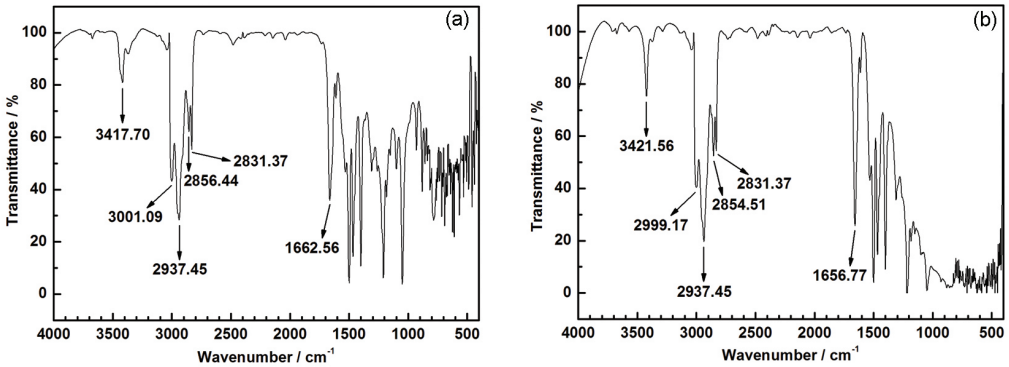

Fig. S40 FTIR spectra of (a) **2a** and (b) **2b** in $CHCl_3$ at a concentration of 100 mM, respectively.

*^{1}H NMR spectra of **2b** in $CDCl_3$/DMSO-d_6*

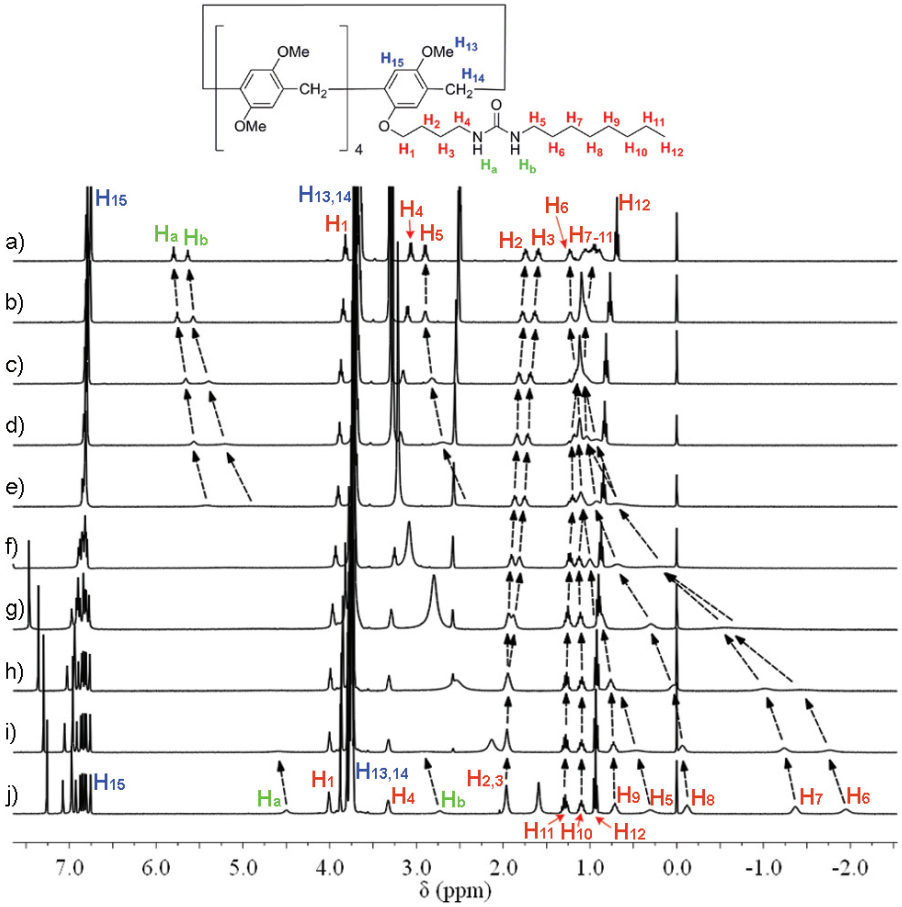

Fig. S41 ^{1}H NMR spectra (400 MHz, 298 K) of **2b** (8 mM) in (a) DMSO-d_6, (b) $CDCl_3$/75% DMSO-d_6 (v/v for all cases), (c) $CDCl_3$/50% DMSO-d_6, (d) $CDCl_3$/40% DMSO-d_6, (e) $CDCl_3$/30% DMSO-d_6, (f) $CDCl_3$/20% DMSO-d_6, (g) $CDCl_3$/10% DMSO-d_6, (h) $CDCl_3$/5% DMSO-d_6, (i) $CDCl_3$/2% DMSO-d_6, and (j) $CDCl_3$.

*^{1}H NMR spectra of **1c**, **1b**, and **2b** with the addition of anions*

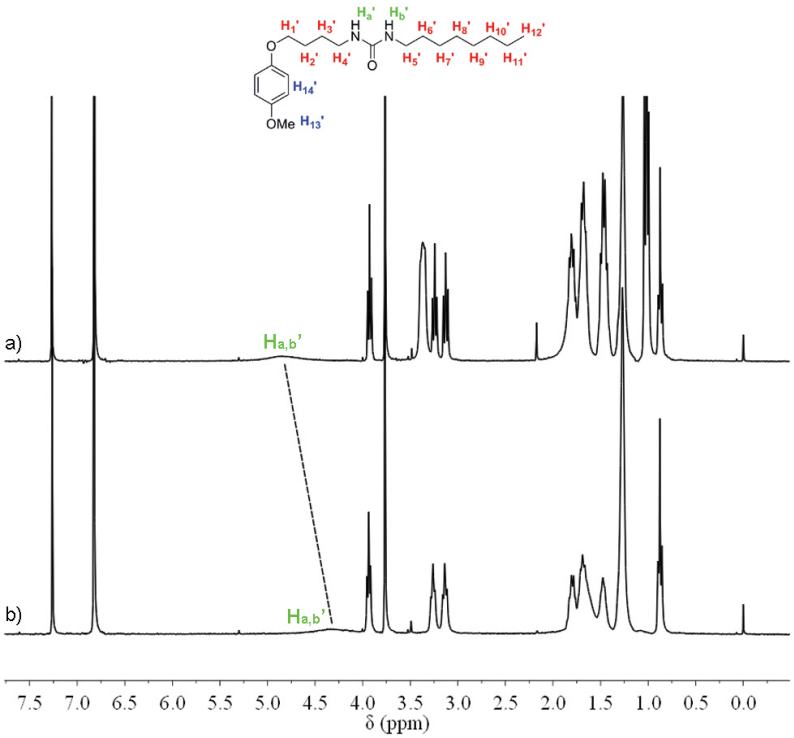

Fig. S42 ^{1}H NMR spectra (300 MHz, $CDCl_3$, 298 K) of **1c** (10 mM) with the addition of Cl^- (TBA^+): (a) 1.0 equiv and (b) 0 equiv.

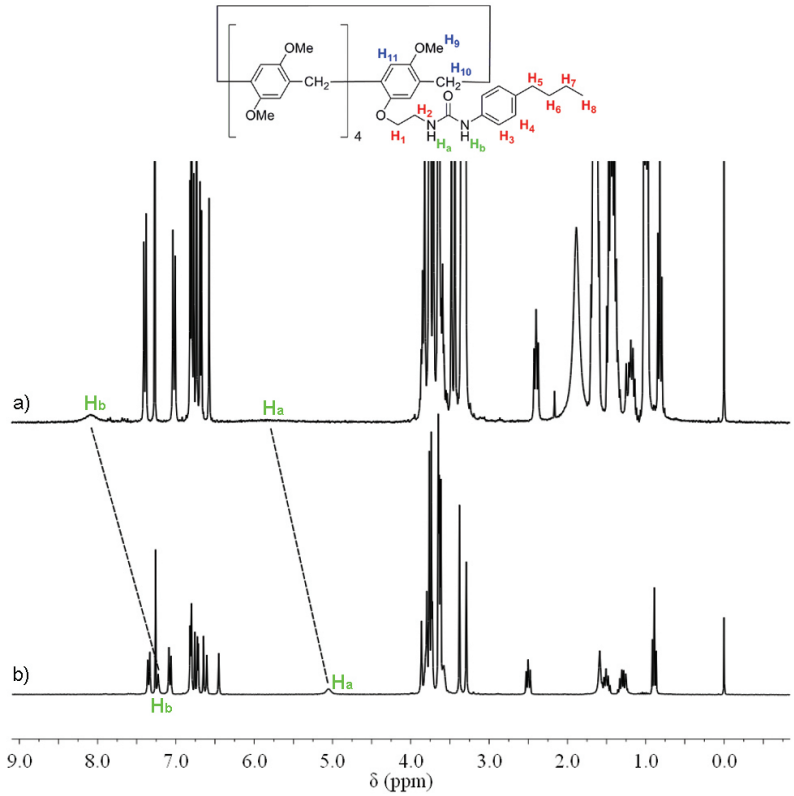

Fig. S43 ^{1}H NMR spectra (300 MHz, $CDCl_3$, 298 K) of **1b** (10 mM) with the addition of Cl^- (TBA^+): (a) 1.9 equiv and (b) 0 equiv.

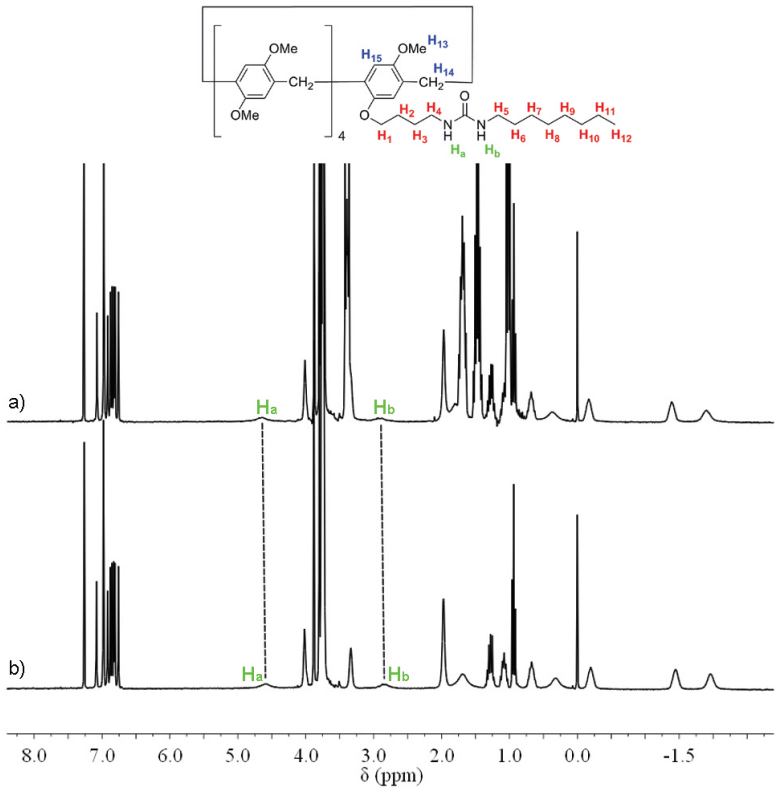

Fig. S44 ^{1}H NMR spectra (300 MHz, $CDCl_3$, 298 K) of **2b** (10 mM) with the addition of Br^- (TBA^+): (a) 1.5 equiv and (b) 0 equiv.

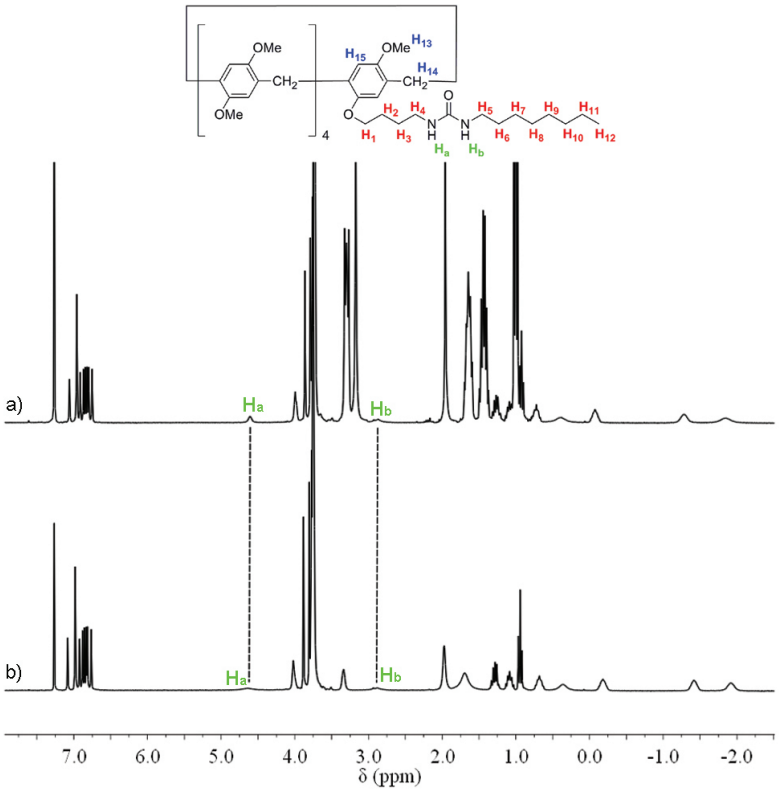

Fig. S45 ^{1}H NMR spectra (300 MHz, $CDCl_3$, 298 K) of **2b** (10 mM) with the addition of AcO^- (TBA^+): (a) 2.5 equiv and (b) 0 equiv.

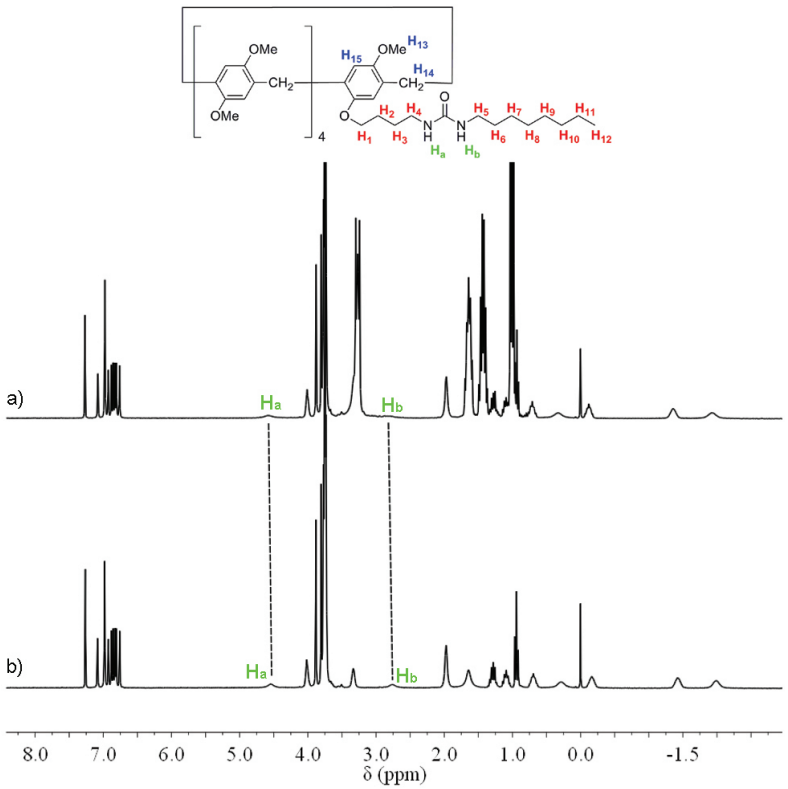

Fig. S46 ^{1}H NMR spectra (300 MHz, $CDCl_3$, 298 K) of **2b** (10 mM) with the addition of CF_3COO^- (TBA^+): (a) 2.1 equiv and (b) 0 equiv.

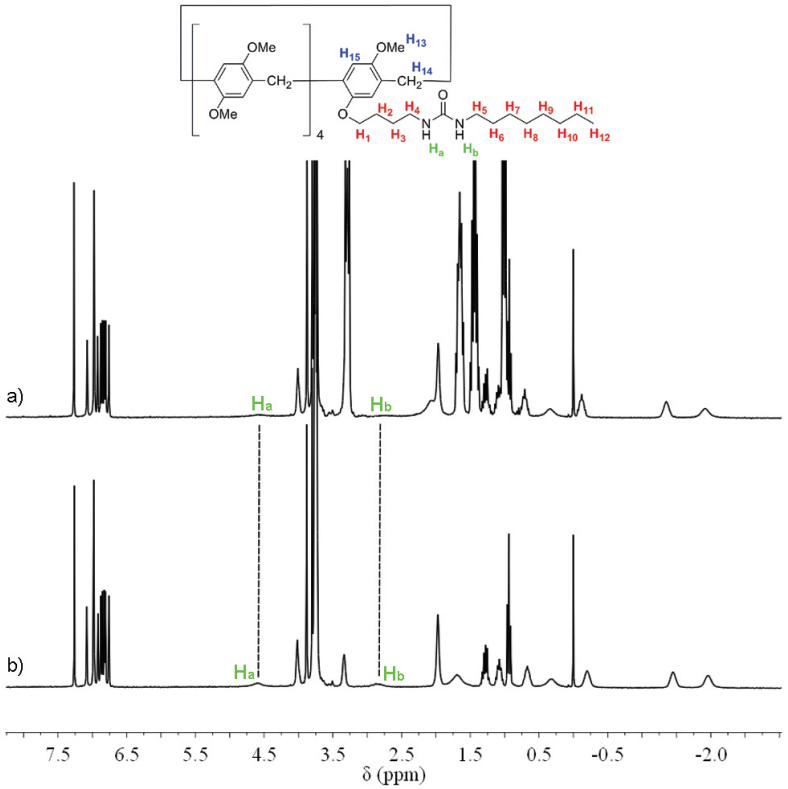

Fig. S47 ^{1}H NMR spectra (300 MHz, $CDCl_3$, 298 K) of **2b** (10 mM) with the addition of NO_3^- (TBA^+): (a) 2.0 equiv and (b) 0 equiv.

*Crystal structure and crystal data of **2a***

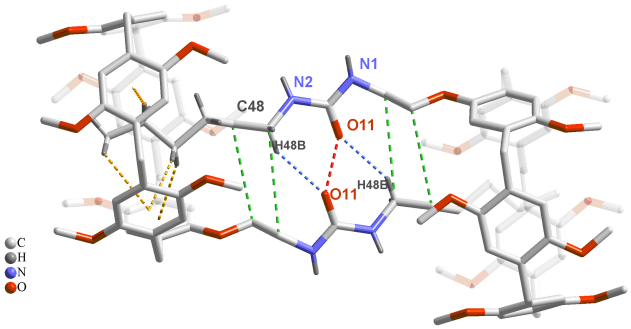

Fig. S48 Crystal structure of the [c2]daisy chain formed by **2a**.[S6] Hydrogen atoms and solvent molecules that are not involved in hydrogen bonding (except for urea protons) have been omitted for clarity. There are three kinds of typical hydrogen bonds, C–H···π interactions (omitted in another cavity for symmetry), C–H···O=C interactions and van der waals interactions, represented by yellow, blue and green dotted lines, respectively. The distances of H···ring centre were in the range of 2.33–3.13 Å for C–H···π interactions. The distances of H···O were 2.49 Å for C–H···O=C interactions. And the distances between two carbon atoms were in the range of 3.97–4.12 Å for van der waals interactions. Specially, the possible secondary bonding was represented by a red dotted line, with the O···O distance 2.44 Å and the angle of O···O=C 135°.

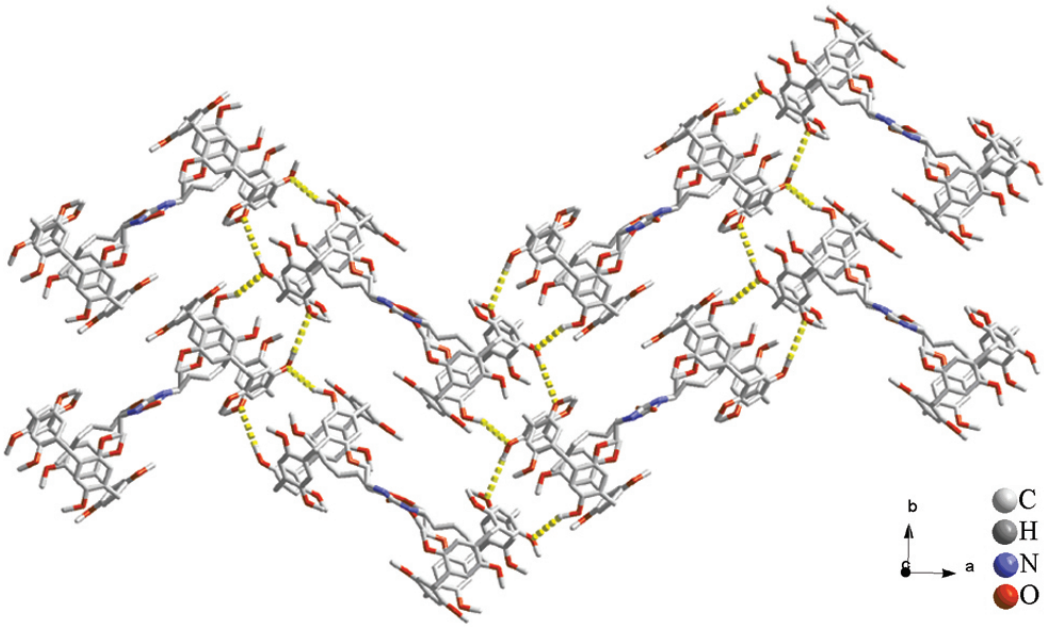

Fig. S49 Packing plot of **2a** in the solid state showing the C–H···O interactions between [c2]daisy chains (yellow dotted lines). The distances of H···O were 2.71–3.13 Å for C–H···O interactions. Hydrogen atoms and solvent molecules are omitted for clarity.

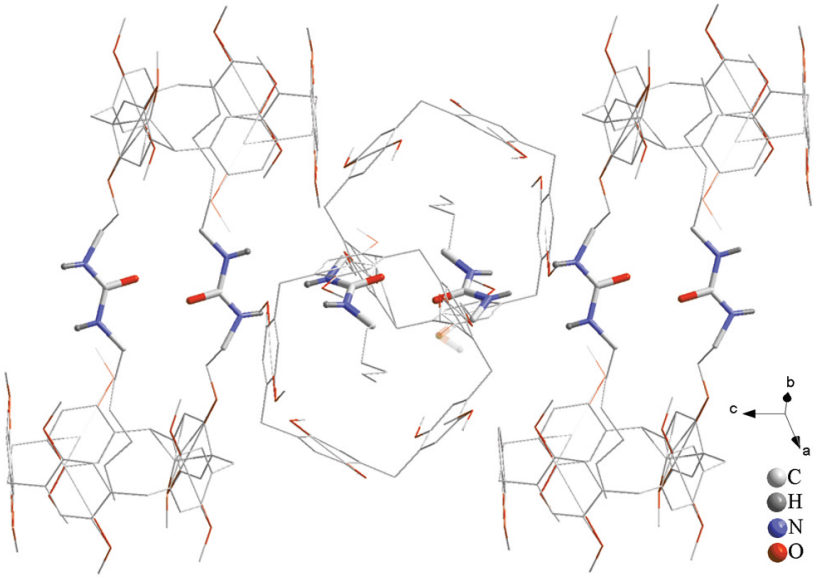

Fig. S50 Packing plot of **2a** in the solid state showing the cross stacking of [c2]daisy chains and no hydrogen bonding for NH. Hydrogen atoms except for the ureido groups and solvent molecules are omitted for clarity.

Table S2 Crystal data and structure refinement for **2a**

CCDC number	947531
Empirical formula	$C_{216}H_{274}Cl_8N_8O_{45}$
Formula weight	3986.03
Temperature	296(2)
Wavelength	0.71073 Å
Crystal system	monoclinic
Space group	*C2/c*
a	40.0942(14) Å
b	14.3501(12) Å
c	20.0274(15) Å
α	90.00°
β	107.931(3)°
γ	90.00°
Volume	10963.2(13) $Å^3$
Z	2
Density (calculated)	1.207
Absorption coefficient	0.177
F(000)	4244
Crystal size	0.24 × 0.20 × 0.18 mm^3
Theta range for data collection	2.16 to 26.00°
Index ranges	−49<=h<=48, −17<=k<=17, −24<=l<=23
Reflections collected	10618
Independent reflections	5399 [R(int) = 0.0379]
Completeness to theta = 26.00°	98.4 %
Absorption correction	multi-scan
Refinement method	Full-matrix least-squares on F^2
Goodness-of-fit on F^2	1.014
Final *R* indices [$I > 2\text{sigma}(I)$]	$R1 = 0.0444$, $wR2 = 0.1062$
R indices (all data)	$R1 = 0.0722$, $wR2 = 0.1082$
Largest diff. peak and hole	0.299 and −0.239 e·$Å^{-3}$

*Optimized structure of **2a***

The self-complexation structure of **2a** is more rigid than that of **2b** because of the shorter alkyl chain length of **2a**. Therefore, we selected **2a** as the example for the theoretical calculations. Using the density functional theory (DFT) method, the self-complexation structure of **2a** was optimized. The geometry optimizations were carried out in gas phase, at the M062X/6-31G (d, p) level by employing the Gaussian09 program.[S7] The results are shown in Fig. S51, where the ureas adopt different orientations of the N−H bonds in the two conformations. And the energy of conformation b is only 6.1 kJ/mol higher than that of conformation a, which means that conformation a is a little more stable.

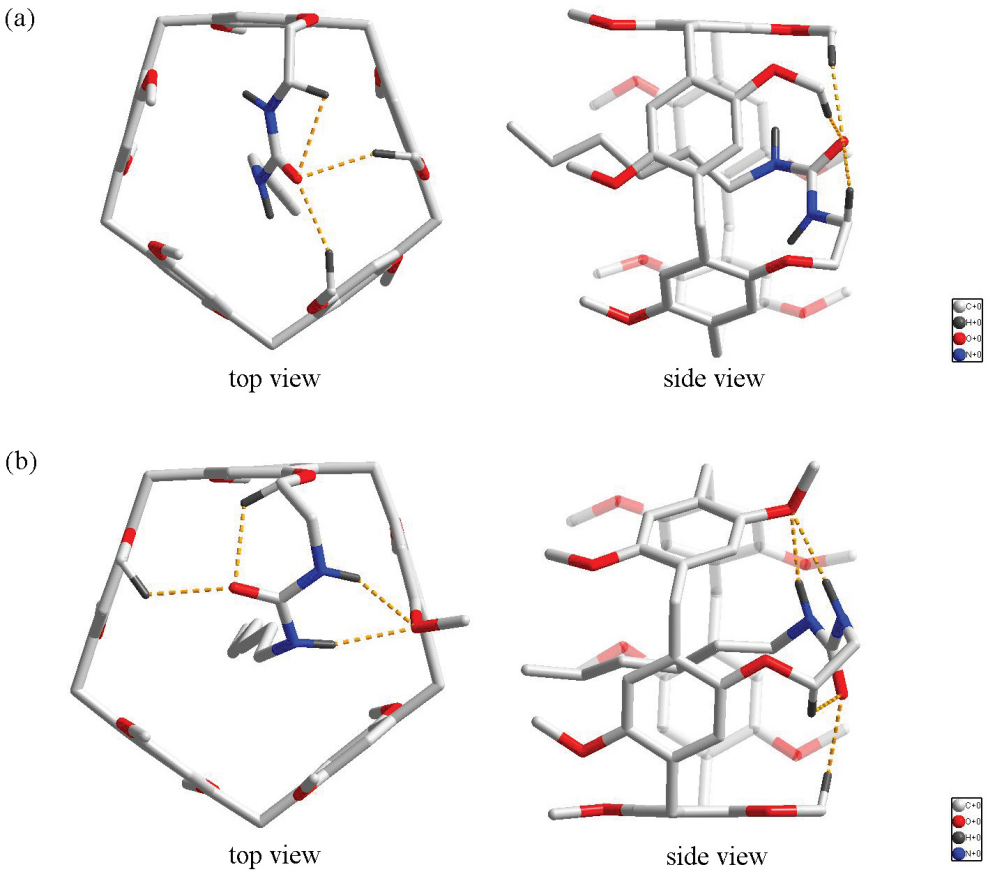

Fig. S51 The optimized self-complexation structures of **2a** in two conformations with two N−H bonds of the ureas oriented in the (a) opposite direction and (b) same direction. Hydrogen atoms that are not involved in hydrogen bonding (except for urea protons) have been omitted for clarity. The yellow dotted lines stand for hydrogen bonds. The calculated energies of the optimized geometries for the two conformations are different and the ΔE is about −6.1 kJ/mol ($E_a - E_b$).

References

S1 G. M. Sheldrick, *SHELXL-97: Crystal Structure Refinement*, University of Göttingen, Göttingen, Germany, 1997.

S2 (a) D. M. Schultz, J. A. Prescher, S. Kidd, D. Marona-Lewicka, D. E. Nichols and A. Monte, *Bioorg. Med. Chem.*, 2008, **16**, 6242−6251; (b) Y. Li, G. Li, X. Wang, C. Lin, Y. Zhang and Y. Ju, *Chem.–Eur. J.*, 2008, **14**, 10331−10339.

S3 L. Liu, D. Cao, Y. Jin, H. Tao, Y. Kou and H. Meier, *Org. Biomol. Chem.*, 2011, **9**, 7007−7010.

S4 N. L. Strutt, R. S. Forgan, J. M. Spruell, Y. Y. Botros and J. F. Stoddart, *J. Am. Chem. Soc.*, 2011, **133**, 5668−5671.

S5 T. Ogoshi, S. Kanai, S. Fujinami, T.-A. Yamagishi and Y. Nakamoto, *J. Am. Chem. Soc.*, 2008, **130**, 5022−5023.

S6 Here are some examples that the supramolecular structures in solution were not consistent with the case in solid state. See: (a) F. Wang, Q. Zhou, K. Zhu, S. Li, C. Wang, M. Liu, N. Li, F. R. Fronczek and F. Huang, *Tetrahedron*, 2009, **65**, 1488–1494; (b) F. Zapata, A. Caballero, N. G. White, T. D. W. Claridge, P. J. Costa, V. Félix and P. D. Beer, *J. Am. Chem. Soc.*, 2012, **134**, 11533−11541; (c) M. Wei, B. Wu, L. Zhao, H. Zhang, S. Li, Y. Zhao and X.-J. Yang, *Org. Biomol. Chem.*, 2012, **10**, 8758−8761.

S7 M. J. Frisch, G. W. Trucks, H. B. Schlegel, G. E. Scuseria, M. A. Robb, J. R. Cheeseman, G. Scalmani, V. Barone, B. Mennucci, G. A. Petersson, H. Nakatsuji, M. Caricato, X. Li, H. P. Hratchian, A. F. Izmaylov, J. Bloino, G. Zheng, J. L. Sonnenberg, M. Hada, M. Ehara, K. Toyota, R. Fukuda, J. Hasegawa, M. Ishida, T. Nakajima, Y. Honda, O. Kitao, H. Nakai, T. Vreven, J. A. Montgomery, Jr., J. E. Peralta, F. Ogliaro, M. Bearpark, J. J. Heyd, E. Brothers, K. N. Kudin, V. N. Staroverov, T. Keith, R. Kobayashi, J. Normand, K. Raghavachari, A. Rendell, J. C. Burant, S. S. Iyengar, J. Tomasi, M. Cossi, N. Rega, J. M. Millam, M. Klene, J. E. Knox, J. B. Cross, V. Bakken, C. Adamo, J. Jaramillo, R. Gomperts, R. E. Stratmann, O. Yazyev, A. J. Austin, R. Cammi, C. Pomelli, J. W. Ochterski, R. L. Martin, K. Morokuma, V. G. Zakrzewski, G. A. Voth, P. Salvador, J. J. Dannenberg, S. Dapprich, A. D. Daniels, O. Farkas, J. B. Foresman, J. V. Ortiz, J. Cioslowski, and D. J. Fox. Gaussian 09, Revision B.01; Gaussian, Inc., Wallingford CT, 2010.1.